FEMS Yeast Research, 18, 2018, foy056

doi: 10.1093/femsyr/foy056
Advance Access Publication Date: 15 May 2018
Research Article

RESEARCH ARTICLE

Laboratory evolution for forced glucose-xylose co-consumption enables identification of mutations that improve mixed-sugar fermentation by xylose-fermenting *Saccharomyces cerevisiae*

Ioannis Papapetridis[#], Maarten D. Verhoeven[#], Sanne J. Wiersma, Maaike Goudriaan, Antonius J.A. van Maris[†] and Jack T. Pronk[*]

Delft University of Technology, Department of Biotechnology, Van der Maasweg 9, 2629 HZ Delft, The Netherlands

[*]**Corresponding author:** Industrial Microbiology Section, Department of Biotechnology, Delft University of Technology, Van der Maasweg 9, 2629 HZ Delft, The Netherlands. Tel: +31 15 2783214; E-mail: j.t.pronk@tudelft.nl
[#]The authors have contributed equally and should be considered as joint first authors.
[†]**Current address:** School of Engineering Sciences in Chemistry, Biotechnology and Health, Department of Industrial Biotechnology, KTH Royal Institute of Technology, AlbaNova University Centre, SE 10691 Stockholm, Sweden
One sentence summary: This article describes a novel laboratory evolution approach to select for mutations that enable decreased fermentation times in second-generation bioethanol production processes with the yeast *Saccharomyces cerevisiae*.
Editor: Jens Nielsen

ABSTRACT

Simultaneous fermentation of glucose and xylose can contribute to improved productivity and robustness of yeast-based processes for bioethanol production from lignocellulosic hydrolysates. This study explores a novel laboratory evolution strategy for identifying mutations that contribute to simultaneous utilisation of these sugars in batch cultures of *Saccharomyces cerevisiae*. To force simultaneous utilisation of xylose and glucose, the genes encoding glucose-6-phosphate isomerase (*PGI1*) and ribulose-5-phosphate epimerase (*RPE1*) were deleted in a xylose-isomerase-based xylose-fermenting strain with a modified oxidative pentose-phosphate pathway. Laboratory evolution of this strain in serial batch cultures on glucose–xylose mixtures yielded mutants that rapidly co-consumed the two sugars. Whole-genome sequencing of evolved strains identified mutations in *HXK2*, *RSP5* and *GAL83*, whose introduction into a non-evolved xylose-fermenting *S. cerevisiae* strain improved co-consumption of xylose and glucose under aerobic and anaerobic conditions. Combined deletion of *HXK2* and introduction of a $GAL83^{G673T}$ allele yielded a strain with a 2.5-fold higher xylose and glucose co-consumption ratio than its xylose-fermenting parental strain. These two modifications decreased the time required for full sugar conversion in anaerobic bioreactor batch cultures, grown on 20 g L^{-1} glucose and 10 g L^{-1} xylose, by over 24 h. This study demonstrates that laboratory evolution and genome resequencing of microbial strains engineered for forced co-consumption is a powerful approach for studying and improving simultaneous conversion of mixed substrates.

Keywords: biofuels; yeast; industrial biotechnology; redox engineering; fermentation; pentoses

Received: 14 February 2018; **Accepted:** 14 May 2018

INTRODUCTION

Industrial biotechnology can contribute to reconciliating global demands for liquid transport fuels with the almost universally accepted need to limit anthropogenic CO_2 emissions (Fulton *et al.* 2015). Bioethanol, the biofuel with the largest annual global production volume, is still predominantly produced by fermentation of sucrose or glucose, derived from sugar cane or corn starch, respectively (Gombert and van Maris 2015). These 'first-generation' bioethanol processes exploit the natural high fermentation rates and ethanol yield of the yeast *Saccharomyces cerevisiae*. Optimisation of yeast strains and production processes enables many industrial processes to operate at >90% of the theoretical ethanol yield on sugar (Basso, Basso and Nitsche Rocha 2011; Gombert and van Maris 2015; Lopes *et al.* 2016). However, the massive scaling up of production volumes that would be required to replace a substantial fraction of petroleum-based transport fuels cannot be sustainably achieved with corn starch and cane sugar as the only feedstocks. Instead, a large fraction of the feedstock will have to be derived from lignocellulosic plant biomass, such as agricultural residues and energy crops (Lynd *et al.* 2017).

In comparison with first-generation feedstocks, lignocellulosic hydrolysates pose additional challenges for yeasts and yeast researchers. In addition to containing mixtures of hexose and pentose (mainly D-xylose and L-arabinose) sugars, the deconstruction of lignocellulosic biomass that precedes yeast-based fermentation releases fermentation inhibitors (Palmqvist and Hahn-Hägerdal 2000; van Maris *et al.* 2006; Jansen *et al.* 2017). Intensive metabolic engineering studies, encompassing functional expression of heterologous pathways for xylose and arabinose catabolism, improvements in inhibitor tolerance and minimisation of by-product formation have yielded *S. cerevisiae* strains that are now applied in the first full-scale 'second-generation' industrial bioethanol plants (Moysés *et al.* 2016; Jansen *et al.* 2017). However, further improvements in ethanol titres, yields and productivities are important to increase the economic viability of this nascent technology.

Current strain engineering strategies for enabling pentose fermentation by *S. cerevisiae* typically yield strains that, in anaerobic batch cultures grown on sugar mixtures, preferentially ferment glucose, while xylose and/or arabinose are predominantly converted in a second, slower fermentation phase (Jansen *et al.* 2017). This strong preference for glucose over pentoses persists even after extensive laboratory evolution on sugar mixtures (Kuyper *et al.* 2005b; Wisselink *et al.* 2009; Garcia Sanchez *et al.* 2010; Shen *et al.* 2012; Zhou *et al.* 2012). Achieving efficient co-fermentation of glucose and pentoses, while maintaining a high overall rate of sugar conversion, could increase volumetric productivity of industrial processes. Moreover, since several inhibitors of yeast performance are more harmful during the slower pentose fermentation phase (Bellissimi *et al.* 2009; Kim *et al.* 2012; Ask *et al.* 2013; Jansen *et al.* 2017), simultaneous fermentation of glucose and pentose sugars can also contribute to robustness under industrial process conditions.

Random mutagenesis, laboratory evolution and protein engineering of xylose transporters have yielded transporter variants with improved xylose affinity and reduced glucose inhibition, which enabled the construction of yeast strains with improved xylose consumption in the presence of glucose (Farwick *et al.* 2014; Nijland *et al.* 2014; Reznicek *et al.* 2015; Shin *et al.* 2015). In an alternative approach, expression of a heterologous cellodextrin transporter and an intracellular β-glucosidase, along with a heterologous xylose reductase/xylitol dehydrogenase (XR/XDH) pathway, enabled simultaneous consumption of cellobiose and xylose in *S. cerevisiae* by reducing the impact of glucose repression (Wei *et al.* 2015). However, despite progress in this area, engineering of yeast strains showing simultaneous, fast fermentation of glucose and xylose remains a key challenge.

Deletion of *RPE1*, which encodes the pentose-phosphate-pathway (PPP) enzyme ribulose-5-phosphate epimerase, was recently shown to result in coupling of glucose and xylose catabolism, at a ratio of 10:1, in an engineered xylose-utilising *S. cerevisiae* strain (Shen *et al.* 2015). Despite a low xylose-to-glucose consumption ratio, this strategy indicated the potential of forced stoichiometric coupling of glucose and pentose metabolism in *S. cerevisiae*. In *S. cerevisiae*, phosphoglucose isomerase (Pgi1) catalyses interconversion of glucose-6-phosphate to fructose-6-phosphate in upper glycolysis (Aguilera 1986). Since deletion of *PGI1* blocks glycolysis, *pgi1*Δ strains cannot grow on glucose as the sole carbon source unless all glucose-6-phosphate is rerouted through the PPP. Deletion of *eda*, *rpe* and *pgi* in *Escherichia coli* was previously shown to enable co-consumption of xylose and glucose (Gawand *et al.* 2013). As conversion of 1 mol glucose-6-phosphate to 1 mol ribulose-5-phosphate via the oxidative branch of the PPP results in a net generation of 2 mol NADPH, the absence of a redox imbalance relied on conversion of excess NADPH to NADH by the native *E. coli* transhydrogenases.

Wild-type *S. cerevisiae* strains cannot reoxidise all NADPH generated by such a redirection of metabolism and, consequently, *pgi1*-null mutants cannot grow on glucose as sole carbon source (Boles, Lehnert and Zimmermann 1993; Dickinson, Sobanski and Hewlins 1995). Overexpression of *GDH2*, which encodes NAD^+-dependent glutamate dehydrogenase, can restore growth of *pgi1*Δ strains by enabling a transhydrogenase-like cycle that couples the interconversion of 2-oxoglutarate and glutamate to the conversion of NADPH and NAD^+ to $NADP^+$ and NADH (Boles, Lehnert and Zimmermann 1993). Based on the impact of a *pgi1*Δ mutation on glucose metabolism, we reasoned that inactivation of *PGI1* might be used to construct strains with a stringent requirement for co-utilisation of xylose and glucose, at much higher ratios than hitherto demonstrated.

The goal of this study was to explore a new strategy for identifying mutations that stimulate glucose-xylose co-consumption by *S. cerevisiae*. The strategy was based on enforcing a strict stoichiometric coupling of glucose and xylose fermentation by the combined deletion of *RPE1* and *PGI1* in an engineered, xylose-isomerase-based *S. cerevisiae* strain (Kuyper *et al.* 2005a; Verhoeven *et al.* 2017). Furthermore, to reduce the impact of these modifications on $NADP^+$/NADPH redox cofactor balancing, the native $NADP^+$-dependent 6-phosphogluconate dehydrogenases (Gnd1 and Gnd2) were replaced by a heterologous NAD^+-dependent enzyme (Papapetridis *et al.* 2016). After laboratory evolution for improved growth on glucose-xylose mixtures, the physiology of evolved strains was analysed in aerobic shake-flask and bioreactor batch cultures. Potential causal mutations identified by whole-genome sequencing were introduced into a non-evolved (*PGI1 RPE1 GND1 GND2*) xylose-fermenting strain background. The resulting reverse engineered strains were then analysed in shake-flask and anaerobic bioreactor batch cultures, grown on mixtures of glucose and xylose.

Table 1. Strains used in this study.

Strain name	Relevant Genotype	Origin
CEN.PK113–7D	*MATa MAL2–8c SUC2 CAN1*	Entian and Kötter (2007)
IMX581	*MATa ura3–52 MAL2–8c SUC2 can1::cas9-natN2*	Mans *et al.* (2015)
IMX705	*MATa MAL2–8c SUC2 can1::cas9-natNT2 gnd2Δ gnd1::gndA*	Papapetridis *et al.* (2016)
IMX1046	*MATa MAL2–8c SUC2 can1::cas9-natNT2 gnd2Δ gnd1::gndA gre3::ZWF1, SOL3, TKL1, TAL1, NQM1, RKI1, TKL2 sga1::9∗xylA, XKS1 rpe1Δ pgi1Δ*	This work
IMX994	*MATa ura3–52 MAL2–8c SUC2 can1::cas9-natN2, gre3::RPE1, TKL1, TAL1, RKI1, XKS1*	This work
IMU079	*MATa ura3–52 MAL2–8c SUC2 can1::cas9-natN2, gre3::RPE1, TKL1, TAL1, RKI1, XKS1* pAKX002	This work
IMX1485	*MATa ura3–52 MAL2–8c SUC2 gre3::RPE1, TKL1, TAL1, RRKI1, XKS1 hxk2Δ* pAKX002	This work
IMX1486	*MATa ura3–52 MAL2–8c SUC2 gre3::RPE1, TKL1, TAL1, RKI1, XKS1 gal83Δ* pAKX002	This work
IMX1487	*MATa ura3–52 MAL2–8c SUC2 gre3::RPE1, TKL1, TAL1, RKI1, XKS1 rsp5Δ* pAKX002	This work
IMX1488	*MATa ura3–52 MAL2–8c SUC2 gre3::RPE1, TKL1, TAL1, RKI1, XKS1 gal83::GAL83^{G673T}* pAKX002	This work
IMX1515	*MATa ura3–52 MAL2–8c SUC2 gre3::RPE1, TKL1, TAL1, RKI1, XKS1 rsp5Δ hxk2Δ* pAKX002	This work
IMX1583	*MATa ura3–52 MAL2–8c SUC2 gre3::RPE1, TKL1, TAL1, RKI1, XKS1 gal83::GAL83^{G673T} hxk2Δ* pAKX002	This work

MATERIALS AND METHODS

Maintenance of strains

The CEN.PK lineage of *S. cerevisiae* laboratory strains (Entian and Kötter 2007) was used to construct and evolve all strains used in this study (Table 1, Additional File 1). Depending on strain auxotrophies, cultures were grown in YP (10 g L^{-1} yeast extract, 20 g L^{-1} peptone) (BD, Franklin Lakes, NJ) or synthetic medium (SM) (Verduyn *et al.* 1992), supplemented with glucose (20 g L^{-1}), xylose (20 g L^{-1}), a glucose/xylose mixture (10 g L^{-1} of each sugar) or a xylose/fructose/glucose mixture (20, 10 and 1 g L^{-1} respectively). Propagation of *E. coli* XL-1 Blue cultures was performed in LB medium (5 g L^{-1} Bacto yeast extract, 10 g L^{-1} Bacto tryptone, 5 g L^{-1} NaCl, 100 μg mL^{-1} ampicillin). Frozen stock cultures were stored at –80°C, after addition of glycerol (30% v/v final concentration).

Construction of plasmids and cassettes

PCR amplification for construction of plasmid fragments and yeast integration cassettes was performed with Phusion High Fidelity DNA Polymerase (Thermo-Scientific, Waltham, MA), according to the manufacturer's guidelines. Plasmid assembly was performed *in vitro* with a Gibson Assembly Cloning kit (New England Biolabs, Ipswich, MA), following the supplier's guidelines, or *in vivo* by transformation of plasmid fragments into yeast cells (Kuijpers *et al.* 2013). For all constructs, correct assembly was confirmed by diagnostic PCR with DreamTaq polymerase (Thermo-Scientific), following the manufacturer's protocol. Plasmids used and constructed in this work are described in Additional File 2. All yeast genetic modifications were performed using CRISPR/Cas9-based genome editing (Mans *et al.* 2015). Unique guide-RNA (gRNA) sequences targeting *GRE3*, *GAL83* and *RSP5* were selected from a publicly available list (DiCarlo *et al.* 2013) and synthesised (Baseclear, Leiden, The Netherlands). Primers and oligonucleotides used in this work are listed in Additional File 3.

To construct the *GRE3*-targeting CRISPR-plasmid pUDR204, the plasmid backbone of pMEL11 was PCR amplified using primer combination 5980/5792. The insert fragment, expressing the *GRE3*-targeting gRNA, was amplified using primer combination 5979/5978 and pMEL11 as template. To construct the *RPE1*/*PGI1* double-targeting CRISPR-plasmid pUDR202, the plasmid backbone and the insert fragment were PCR amplified using primer combinations 5941/6005 and 9269/9401, respectively, using pROS11 as template. Both plasmids were assembled *in vitro* and cloned in *E. coli*. To construct CRISPR-plasmids for single deletion of *GAL83* and *RSP5*, the plasmid backbone, the *GAL83*-gRNA insert and the *RSP5*-gRNA insert were amplified using primer combination 5792/5980, 5979/11 270 and 5979/11 373, respectively, using pMEL10 as template and assembled *in vivo*.

To generate *ZWF1* and *SOL3* overexpression cassettes, promoter regions of *ADH1* and *ENO1* and the coding regions of *ZWF1* and *SOL3* (including their terminator regions) were PCR amplified using primer combinations 8956/8960, 8958/8961, 8953/8964 and 8984/8986, respectively, using CEN.PK113–7D genomic DNA as a template. The resulting products were used as templates for fusion-PCR assembly of the p*ADH1*-*ZWF1*-t*ZWF1* and p*ENO1*-*SOL3*-t*SOL3* overexpression cassettes with primer combinations 8956/8964 and 8958/8986, respectively, which yielded plasmids pUD426 and pUD427 after ligation to pJET-blunt vectors (Thermo-Scientific) and cloning in *E. coli*.

To generate yeast-integration cassettes for overexpression of the major genes of the complete PPP, p*ADH1*-*ZWF1*-t*ZWF1*, p*ENO1*-*SOL3*-t*SOL3*, p*PGK1*-*TKL1*-t*TKL1*, p*TEF1*-*TAL1*-t*TAL1*, p*PGI1*-*NQM1*-t*NQM1*, p*TPI1*-*RKI1*-t*RKI1* and p*PYK1*-*TKL2*-t*TKL2* cassettes were PCR amplified using primer combinations 4870/7369, 8958/3290, 3291/4068, 3274/3275, 3847/3276, 4691/3277 and 3283/3288, respectively, using plasmids pUD426, pUD427, pUD348, pUD349, pUD344, pUD345 and pUD346, respectively, as templates. To generate yeast-integration cassettes of the genes of the non-oxidative PPP, the p*TDH3*-*RPE1*-t*RPE1*, p*PGK1*-*TKL1*-t*TKL1*, p*TEF1*-*TAL1*-t*TAL1*, p*TPI1*-*RKI1*-t*RKI1* overexpression cassettes were PCR-amplified using primer pairs 7133/3290, 3291/4068, 3724/3725 and 10 460/10 461, respectively and plasmids pUD347, pUD348, pUD34 and pUD345 as templates.

Yeast-integration cassettes for overexpression of *Piromyces* sp. xylose isomerase (p*TPI1*-*xylA*-t*CYC1*) were PCR-amplified using primer combinations 6285/7548, 6280/6273, 6281/6270, 6282/6271, 6284/6272, 6283/6275, 6287/6276, 6288/6277 or 6289/6274, using pUD350 as template. Yeast xylulokinase overexpression cassettes (p*TEF1*-*XKS1*-t*XKS1*) were PCR-amplified from plasmid pUD353, using primer combination 5920/9029 or 7135/7222. A yeast-integration cassette of p*GAL83*-*gal83*::*GAL83^{G673T}*-t*GAL83* was PCR-amplified from genomic DNA of IMS0629, using primer combination 11 273/11 274.

Strain construction

Yeast transformation was performed as previously described (Gietz and Woods 2002). Transformation mixtures were plated on SM or YP agar plates (2% Bacto Agar, BD), supplemented with the appropriate carbon sources. For transformations with the *amdS* marker cassette, agar plates were prepared and counter selection was performed as previously described (Solis-Escalante *et al.* 2013). For transformations with the *URA3* selection marker counterselection was performed using 5-fluoro-orotic acid (Zymo Research, Irvine, CA), following the supplier's protocol. For transformations with the *hphNT* marker, agar plates were additionally supplemented with 200 mg L^{-1} hygromycin B (Invivogen, San Diego, CA) and plasmid loss was induced by cultivation in non-selective medium. After each transformation, correct genotypes were confirmed by diagnostic PCR using DreamTaq polymerase (Thermo-Scientific, see Additional File 3 for primer sequences).

Co-transformation of pUDR204 along with the p*ADH1-ZWF1-tZWF1*, p*ENO1-SOL3-tSOL3*, p*PGK1-TKL1-tTKL1*, p*TEF1-TAL1-tTAL1*, p*PGI1-NQM1-tNQM1*, p*TPI1-RKI1-tRKI1* and p*PYK1-TKL2-tTKL2* integration cassettes to IMX705 (Papapetridis *et al.* 2016) and subsequent plasmid counterselection yielded strain IMX963, which overexpresses the major enzymes of the PPP. Co-transformation of pUDR119, 9 copies of the *pTPI1-xylA-tCYC1* integration cassette, along with a single copy of the *pTEF1-XKS1-tXKS1*cassette, to IMX963 followed by plasmid counterselection yielded the xylose-fermenting strain IMX990. In IMX990, the *pTPI1-xylA-tCYC1* cassettes recombined *in vivo* to form a multicopy construct of xylose isomerase overexpression (Verhoeven *et al.* 2017). To construct IMX1046, in which *RPE1* and *PGI1* were deleted, plasmid pUDR202 and the repair oligonucleotides 9279/9280/9281/9282 were co-transformed to IMX990. Transformation mixes of IMX1046 were plated on SM agar supplemented with a xylose/fructose/glucose mixture (20, 10 and 1 g L^{-1} final concentrations respectively), to avoid potential glucose toxicity (Boles, Lehnert and Zimmermann 1993).

To construct strain IMX994, plasmid pUDE335 was co-transformed to IMX581, along with the p*TDH3-RPE1-tRPE1*, p*PGK1-TKL1-tTKL1*, p*TEF1-TAL1-tTAL1*, p*TPI1-RKI1-tRKI1* and *pTEF1-XKS1-tXKS1* integration cassettes, after which the CRISPR plasmid was recycled. Transformation of pAKX002 to IMX994 yielded the xylose-fermenting strain IMU079. Co-transformation of pUDE327 along with the repair oligonucleotides 5888/5889 to IMX994 yielded strain IMX1384, in which *HXK2* was deleted. Co-transformation of the pMEL10 backbone fragment, along with the *GAL83*-gRNA insert or the *RSP5*-gRNA insert and repair oligonucleotides 11 271/11 272 or 11 374/11 375, respectively, yielded strains IMX1385 (*GAL83* deletion) and IMX1442 (*RSP5* deletion). Counterselection of the CRISPR plasmids from IMX1384, IMX1385 and IMX1442 yielded, respectively, strains IMX1408, IMX1409 and IMX1451. Transformation of pAKX002 to IMX1408, IMX1409 and IMX1451 yielded the xylose-fermenting strains IMX1485, IMX1486 and IMX1487, respectively. To construct strain IMX1453, in which the mutated $GAL83^{G673T}$ gene replaced the wild-type *GAL83* allele, plasmid pUDR105 was co-transformed to IMX1409 with the p*GAL83-gal83*::$GAL83^{G673T}$-t*GAL83* cassette. Transformation of pAKX002 to IMX1453 yielded the xylose-fermenting strain IMX1488. To construct the *hxk2*Δ *rsp5*Δ strain IMX1484, plasmid pUDE327 was co-transformed to IMX1451, along with the repair oligonucleotides 5888/5889. Counterselection of pUDE327 from IMX1484 yielded strain IMX1510. Transformation of pAKX002 to IMX1510 yielded the xylose-fermenting strain IMX1515. To construct the *hxk2*Δ *gal83*::$GAL83^{G673T}$ strain IMX1563, plasmid pUDE327 along with the repair oligonucleotides 5888/5889 was co-transformed to IMX1453. Counterselection of pUDE327 from IMX1563 yielded IMX1571. The xylose-fermenting strain IMX1583 was obtained by transformation of pAKX002 to IMX1571.

Cultivation and media

Shake-flask growth experiments were performed in 500-mL conical shake flasks containing 100 mL of SM with urea as nitrogen source (2.3 g L^{-1} urea, 6.6 g L^{-1} K_2SO_4, 3 g L^{-1} KH_2PO_4, 1 mL L^{-1} trace elements solution (Verduyn *et al.* 1992) and 1 mL L^{-1} vitamin solution (Verduyn *et al.* 1992)) to prevent medium acidification. The initial pH of the medium was set to 6.0 by titration with 2 mol L^{-1} KOH. Depending on the strains grown, different mixtures of carbon sources (glucose/xylose/fructose) were added and media were filter-sterilised (0.2 μm, Merck, Darmstadt, Germany). The temperature was set to 30°C and the shaking speed to 200 rpm in an Innova incubator (New Brunswick Scientific, Edison, NJ). In each case, pre-culture shake flasks were inoculated from frozen stocks. After 8–12 h of growth, exponentially growing cells from the initial shake flasks were used to inoculate fresh cultures that, after 12–18 h of growth, were used as inoculum for the growth experiments to a starting OD_{660} of 0.4–0.5 in the case of shake-flask growth experiments and of 0.2–0.3 in the case of bioreactor cultivation.

Bioreactor cultures were grown on SM (Verduyn *et al.* 1992), supplemented with a glucose/xylose mixture (10 g L^{-1}/20 g L^{-1} for aerobic cultivation or 20 g L^{-1}/10 g L^{-1} for anaerobic cultivation). Sterilisation of the salt solution was performed by autoclaving at 121°C for 20 min. Sugar solutions were sterilised separately by autoclaving at 110°C for 20 min and added to the sterile salt media along with filter-sterilised vitamin solutions. In the case of anaerobic cultivation, media were additionally supplemented with ergosterol (10 mg L^{-1}) and Tween 80 (420 mg L^{-1}). Sterile antifoam C (0.2 g L^{-1}; Sigma-Aldrich, St. Louis, MO) was added to all media used for bioreactor cultivation. Batch cultures were grown in 2-L bioreactors (Applikon, Delft, The Netherlands) with a 1-L working volume, stirred at 800 rpm. Culture pH was maintained at 5.0 by automatic titration with 2 mol L^{-1} KOH. Temperature was maintained at 30°C. Bioreactors were sparged at 0.5 L min^{-1} with either pressurised air (aerobic cultivation) or nitrogen gas (<10 ppm oxygen, anaerobic cultivation). All reactors were equipped with Viton O-rings and Norprene tubing to minimise oxygen diffusion. Evaporation in bioreactor cultures was minimised by cooling the offgas outlet to 4°C.

Laboratory evolution

Laboratory evolution of strain IMX1046 was performed via serial shake-flask cultivation on SM (Verduyn *et al.* 1992). Cultures were grown in 500-mL shake flasks with 100 mL working volume. Growth conditions were the same as described above. Initially, the cultures were grown on a glucose/xylose concentration ratio of 1.0 g L^{-1}/20 g L^{-1}. After growth was observed, exponentially growing cells (0.05 mL of culture) were transferred to SM with a glucose/xylose concentration ratio of 2.0 g L^{-1}/20 g L^{-1}. During subsequent serial transfers, the glucose content was progressively increased as high growth rates were established at each sugar composition, reaching a final glucose/xylose ratio of 20 g L^{-1}/20 g L^{-1}, to increase the selective pressure for alleviation of glucose repression and/or inhibition of xylose conversion. At that point three single colonies were isolated from two replicate

evolution experiments (IMS0628–630 and IMS0634–636, respectively) by plating on SM with 10 g L^{-1} glucose and 20 g L^{-1} xylose. This medium composition supported fast growth on plates during three consecutive restreaks.

Analytical methods

Offgas analysis, biomass dry weight measurements, HPLC analysis of culture supernatants and correction for ethanol evaporation in bioreactor experiments were performed as previously described (Papapetridis *et al.* 2016). Determination of optical density was performed at 660 nm using a Jenway 7200 spectrophotometer (Cole-Palmer, Staffordshire, UK). Yields of products and biomass-specific sugar uptake rates in bioreactor batch cultures were determined as previously described (Wisselink *et al.* 2009; Papapetridis *et al.* 2016). All values are represented as averages ± mean deviation of independent biological duplicate cultures.

In silico determination of sugar uptake

The Yeast v7.6 consensus metabolic model (Aung, Henry and Walker 2013) was used for *in silico* prediction of relative xylose and glucose consumption rates in aerobic bioreactor batch cultures of strain IMS0629. The COBRA v2 toolbox (Becker *et al.* 2007) was used to read the model in MATLAB vR2017b (Mathworks, Natick, MA), supported by the SBML Toolbox v4.1 and the libSBML v5.12 (Hucka *et al.* 2003). The Gurobi v6.5 linear programming solver (Gurobi Optimization Inc, Houston, TX) was installed and used according to the manual provided. The MATLAB script is provided in Additional File 4.

Genome sequencing

Genomic DNA of strains IMS0629 and IMS0634 was isolated from exponentially growing shake-flask cultures on SM (10 g L^{-1} glucose/20 g L^{-1} xylose) with a Qiagen Blood & Cell culture DNA kit (Qiagen, Germantown, MD), according to the manufacturer's specifications. Whole-genome sequencing was performed on an Illumina HiSeq PE150 sequencer (Novogene Company Limited, Hong Kong), as previously described (Papapetridis *et al.* 2018). Sequence data were mapped to the reference CEN.PK113–7D genome (Nijkamp *et al.* 2012), to which the sequences of the p*TPI1-gndA*-tCYC1 and p*TPI1*-xylA-tCYC1 cassettes were manually added. Data processing and chromosome copy number analysis were carried as previously described (Papapetridis *et al.* 2018).

RESULTS

Design of an *S. cerevisiae* strain with a forced, high stoichiometry of xylose and glucose co-consumption

Design of an *S. cerevisiae* strain whose growth depended on extensive co-consumption of xylose and glucose was based on the observation that inactivation of *PGI1* blocks entry of glucose-6-phosphate into glycolysis, while inactivation of *RPE1* prevents entry of ribulose-5-phosphate into the non-oxidative PPP (Fig. 1).

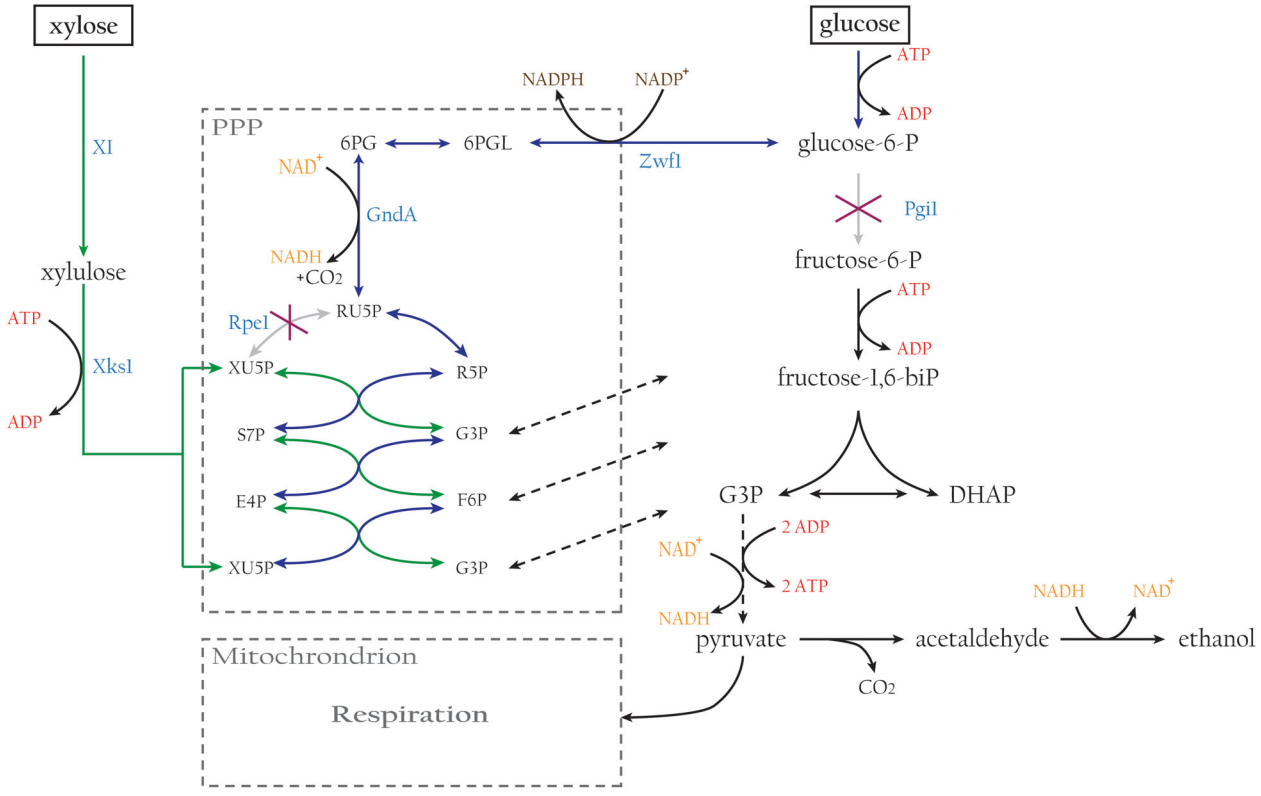

Figure 1. Schematic representation of central carbon metabolism in a yeast strain engineered for forced co-consumption of glucose and xylose. In *pgi1*Δ *rpe1*Δ *S. cerevisiae* expressing a heterologous xylose isomerase (XI, Kuyper *et al.* 2003), the native 6-phosphogluconate dehydrogenases (Gnd1 and Gnd2) were replaced by a bacterial NAD^+-dependent enzyme (GndA, Papapetridis *et al.* 2016). Additionally, xylulokinase (Xks1) and enzymes of the pentose phosphate pathway (PPP) were overexpressed. F6P fructose-6-phosphate; G3P glyceraldehyde-3-phosphate; DHAP dihydroxyacetone phosphate; 6PGL 6-phosphogluconolactone; 6PG 6-phosphogluconate; RU5P ribulose-5-phosphate; XU5P xylulose-5-phosphate; R5P ribose-5-phosphate; S7P sedoheptulose-7-phosphate; E4P erythrose-4-phosphate.

As a consequence, a *pgi1*Δ *rpe1*Δ strain is unable to grow on glucose. If conversion of xylose into xylulose-5-phosphate in such a strain is enabled by expression of a heterologous xylose isomerase and overexpression of the native xylulose kinase Xks1 (Kuyper *et al.* 2005a), co-consumption of xylose and glucose should enable growth (Fig. 1). Overexpression of native genes encoding the enzymes of the non-oxidative PPP has previously been shown to stimulate the required conversion of xylulose-5-phosphate into the glycolytic intermediates fructose-6-phosphate and glyceraldehyde-3-phosphate (Fig. 1) (Johansson and Hahn-Hägerdal 2002; Kuyper *et al.* 2005a). The predicted stoichiometry for conversion of glucose and xylose into pyruvate in a yeast strain that combines these genetic modifications is summarised in Equation 1:

$$\begin{aligned} C_6H_{12}O_6 \; + \; & 2C_5H_{10}O_5 + 5ADP + 5P_i + 2NADP^+ + 5NAD^+ \\ \rightarrow \; & 5C_3H_4O_3 + 5ATP + 4H_2O + 2NADPH + 5NADH \\ + \; & 7H^+ + CO_2 \end{aligned} \quad (1)$$

To prevent a potential excessive formation of NADPH (Boles, Lehnert and Zimmermann 1993; Dickinson, Sobanski and Hewlins 1995), the strain design further included replacement of the native *S. cerevisiae* $NADP^+$-dependent 6-phosphogluconate dehydrogenases (Gnd1 and Gnd2) by the NAD^+-dependent bacterial enzyme GndA (Papapetridis *et al.* 2016), leading to the stoichiometry shown in Equation 2:

$$\begin{aligned} C_6H_{12}O_6 \; + \; & 2\,C_5H_{10}O_5 + 5ADP + 5P_i + 1NADP^+ + 6NAD^+ \\ \rightarrow \; & 5\,C_3H_4O_3 + 5ATP + 4H_2O + NADPH + 6NADH \\ + \; & 7H^+ + CO_2 \end{aligned} \quad (2)$$

As indicated by Equation 2, this strain design forces co-consumption of 2 mol xylose and 1 mol glucose for the production of 5 mol pyruvate, with a concomitant formation of 1 mol NADPH, 6 mol NADH and 5 mol ATP. NADPH generated in this process can be reoxidised in biosynthetic reactions (Bruinenberg, Van Dijken and Scheffers 1983) or via an L-glutamate-2-oxoglutarate transhydrogenase cycle catalysed by Gdh1 and Gdh2 (Boles, Lehnert and Zimmermann 1993). Actual *in vivo* stoichiometries of mixed-sugar consumption will depend on the relative contribution of precursors derived from glucose and xylose to biomass synthesis and on the biomass yield (Verduyn *et al.* 1990). In aerobic cultures, the latter strongly depends on the mode of NADH reoxidation (mitochondrial respiration, alcoholic fermentation and/or glycerol production; Bakker *et al.* 2001). While quantitation of precise co-consumption stoichiometries will therefore require experimental analysis, this strain design clearly has the potential to force xylose and glucose co-consumption at much higher stoichiometries than previously reported (Katahira *et al.* 2008; Shen *et al.* 2012, 2015; Gonçalves *et al.* 2014; Nijland *et al.* 2014; Westman *et al.* 2014; Shin *et al.* 2015).

Construction, laboratory evolution and growth stoichiometry of glucose-xylose co-consuming *S. cerevisiae* strains

To implement the proposed strain design for forced co-consumption of xylose and glucose, multiple copies of a codon-optimised expression cassette for *Piromyces xylA* (Verhoeven *et al.* 2017) were integrated into the genome of *S. cerevisiae* IMX705 (*gnd1*Δ *gnd2*Δ *gndA*; Papapetridis *et al.* 2016), along with overexpression cassettes for *S. cerevisiae XKS1* and for structural genes encoding PPP enzymes. Deletion of *RPE1* and *PGI1* in the resulting xylose-consuming strain IMX990 yielded strain IMX1046, which grew in aerobic shake-flask cultures on SM with 1 g L^{-1} glucose and 20 g L^{-1} xylose as sole carbon sources without a requirement for laboratory evolution. However, this strain did not grow at the same xylose concentration when the glucose concentration was increased to 10 g L^{-1}. Kinetic and/or regulatory constraints in glucose-xylose co-consumption at higher glucose concentrations could, for example, reflect interference of glucose with expression or activity of Hxt transporters involved in xylose uptake.

To select for co-consumption of xylose at higher glucose concentrations, duplicate serial-transfer experiments were performed in aerobic shake-flask cultures on SM with 20 g L^{-1} xylose. During serial transfer, the glucose concentration in the medium was gradually increased from 1 to 20 g L^{-1} (Fig. 2). Samples of the evolving cultures were regularly inoculated in SM containing either 20 g L^{-1} glucose or 20 g L^{-1} xylose as sole carbon source. Absence of growth on these single sugars showed that laboratory evolution did not result in an escape from their forced co-consumption. When, after 13 transfers, vigorous growth was observed on a mixture of 20 g L^{-1} glucose and 20 g L^{-1} xylose, three single-colony isolates were obtained from each laboratory evolution experiment by streaking on SM agar (10 g L^{-1} glucose/20 g L^{-1} xylose).

Growth studies with the six evolved isolates in shake-flask cultures on SM with 10 g L^{-1} glucose and 20 g L^{-1} xylose (Additional File 5) identified isolate IMS0629 (Evolution Line 1) as the fastest growing isolate ($\mu = 0.21\ h^{-1}$). The physiology of this strain was further characterised in aerobic bioreactor batch cultures on SM containing 10 g L^{-1} glucose and 20 g L^{-1} xylose. After a ca. 10-h lag phase (Fig. 3, Additional Files 6 and 7), exponential growth was observed at a specific growth rate of 0.18 h^{-1}. Biomass, ethanol and CO_2 were the main products, with additional minor formation of glycerol and acetate (Table 2, Fig. 3, Additional File 6). During the exponential growth phase, xylose and glucose were co-consumed at a fixed molar ratio of 1.64 mol mol^{-1} (Table 2, Fig. 3). Growth ceased after glucose depletion, at which point xylose consumption rates drastically decreased and corresponded to a simultaneous low rate of xylitol formation (Fig. 3, Additional File 6). As previously reported for XylA-expressing, xylose-fermenting *S. cerevisiae* strains (Kuyper *et al.* 2005a; Verhoeven *et al.* 2017), no production of xylitol was observed during the exponential growth phase. The biomass and ethanol yields on total sugars consumed were 0.28 g biomass (g sugar)$^{-1}$ and 0.18 g ethanol (g sugar)$^{-1}$, respectively. Together with a respiratory quotient of 1.5, these observations indicated a respiro-fermentative sugar dissimilation. In line with the inability of *pgi1*Δ *S. cerevisiae* to generate glucose-6-phosphate from ethanol and acetate, reconsumption of these fermentation products after glucose depletion was not coupled to growth (Fig. 3, Additional File 6). However, their oxidation may have provided redox equivalents for the observed slow production of xylitol from xylose (Fig. 3).

The quantitative data on biomass and product formation obtained from the bioreactor batch cultures enabled a comparison of the observed molar ratio of xylose and glucose consumption with a model-based prediction. To this end, the engineered metabolic network of strain IMX1046 was re-created *in silico*, using the Yeast v7.6 consensus metabolic model as a basis (Aung, Henry and Walker 2013; Additional File 4). Consistent with the

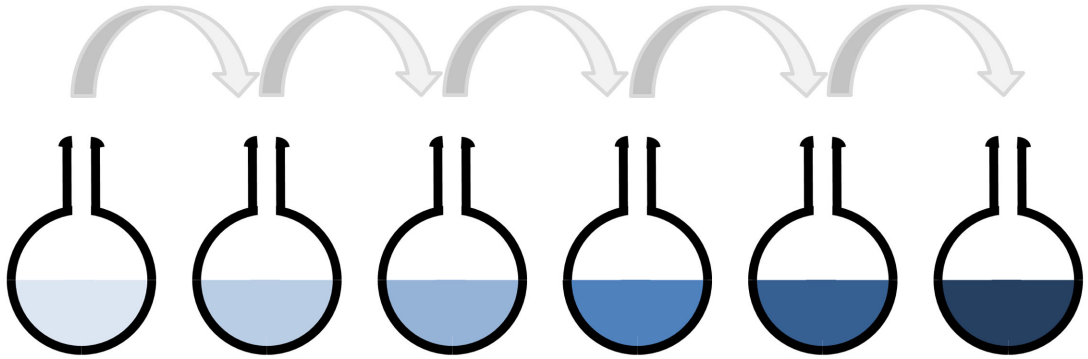

Sugar composition:	20 g L^{-1} xylose 1 g L^{-1} glucose	20 g L^{-1} xylose 2 g L^{-1} glucose	20 g L^{-1} xylose 5 g L^{-1} glucose	20 g L^{-1} xylose 10 g L^{-1} glucose	20 g L^{-1} xylose 10 g L^{-1} glucose	20 g L^{-1} xylose 20 g L^{-1} glucose
Growth after first transfer:	Immediate	Immediate	Observed after 18 or 11 days, respectively	Observed after 9 or 7 days, respectively	Observed after 5 or 3 days, respectively	Observed after 4 days
# of transfers in same medium:	1	1	1	5	2	3

Figure 2. Laboratory evolution of *S. cerevisiae* IMX1046 (*pgi1*Δ *rpe1*Δ *gnd1*Δ *gnd2*Δ *gndA xylA XKS1*↑ PPP↑) for improved co-consumption of xylose at high glucose concentrations. Cultures were grown in shake flasks containing 100 mL SM (pH 6) supplemented with 20 g L^{-1} xylose and progressively increasing glucose concentrations. In every transfer, 0.05 mL of an exponentially growing culture was used to inoculate the next shake flask.

experimental observations on forced co-consumption, inactivation of either xylose or glucose uptake in the model network did not result in any feasible growth solutions. Using the experimentally determined average specific growth rates and oxygen consumption rates from the aerobic bioreactor batch cultures of strain IMS0629 as constraints on the model resulted in predicted xylose and glucose uptake rates of 2.68 and 1.93 mmol (g biomass)$^{-1}$ h^{-1}, respectively, corresponding to a molar ratio of the xylose and glucose consumption rates of 1.4. In view of the complexity of the model and the potential impact of differences in biomass composition, this number corresponded well with the experimentally measured value of 1.64 (Table 2).

Whole-genome sequencing of evolved glucose-xylose co-consuming *S. cerevisiae*

To identify causal mutations for the improved growth of the evolved glucose-xylose co-consuming *S. cerevisiae* strains at high glucose concentrations, the genomes of strains IMS0629 and IMS0634 (fastest growing isolates from evolution line 1 and 2, respectively, Additional File 5) were sequenced and compared to that of their common parental strain. Despite the well-documented role of *S. cerevisiae* hexose transporters in xylose uptake (Reifenberger, Boles and Ciriacy 1997; Hamacher *et al.* 2002; Lee *et al.* 2002; Farwick *et al.* 2014), no mutations were found in the coding region of any of the 18 genes encoding these transporters (*HXT1–17* and *GAL2*), or in other known transporter genes. Both evolved strains harboured mutations in *HXK2* (Table 3). This gene encodes the major *S. cerevisiae* hexokinase which, in addition to its catalytic role, is involved in glucose repression (De Winde *et al.* 1996; Raamsdonk *et al.* 2001). The mutation in IMS0629 caused a premature stop codon at position 309 of Hxk2. Both strains also harboured mutations in *RSP5*, which encodes an E3-ubiquitin ligase linked to ubiquitination and endocytosis of membrane proteins (Belgareh-Touzé *et al.* 2008). In strain IMS0629, a substitution at position 686 caused a glycine to aspartic acid change at position 229 of Rsp5 (Table 3). Strain IMS0634 carried a 41 bp internal deletion in *RSP5*, which included the location of the mutation in strain IMS0629 and probably caused loss of function.

Compared to strain IMS0634, strain IMS0629 harboured four additional nucleotide changes in protein-coding regions (Table 3). A G-A change at position 896 of the transcriptional regulator gene *CYC8* introduced a stop codon at position 299 of the protein. Deletion of *CYC8* was previously shown to enhance xylose uptake in the presence of glucose, albeit at the expense of growth rate (Nijland *et al.* 2017). A G-T change at position 673 of the transcriptional regulator gene *GAL83* caused an amino acid change from aspartic acid to tyrosine at position 225 of the protein. Gal83 plays a vital role in the function of the Snf1-kinase complex of *S. cerevisiae*, which is involved in activation of glucose-repressed genes in the absence of the sugar (Rahner *et al.* 1996; Vincent and Carlson 1998, 1999; Schmidt and McCartney 2000).

Analysis of chromosomal copy number variations showed no chromosomal rearrangements in strain IMS0629 (Additional File 8). In contrast, strain IMS0634 carried a duplication of the right arm of chromosome 3, a duplication of the middle part of chromosome 8 and a duplication of chromosome 9 (Additional File 8). The duplications in chromosomes 8 and 9 in IMS0634 spanned the *GND1*, *GRE3* and *SGA1* loci at which the expressing cassettes for heterologous genes were integrated (Table 1). In the evolved strains IMS0629 and IMS0634, *xylA* copy numbers had increased to ca. 27 and 20, respectively. This observation is consistent with previous research that showed a requirement for high copy numbers of *xylA* expression cassettes to support fast xylose consumption (Alper and Stephanopoulos 2009; Verhoeven *et al.* 2017). The duplication of a segment of chromosome 8 in strain IMS0634 also spanned the locations of the low-to-moderate affinity hexose transporter genes *HXT1* and *HXT5* and the high-affinity hexose transporter gene *HXT4*.

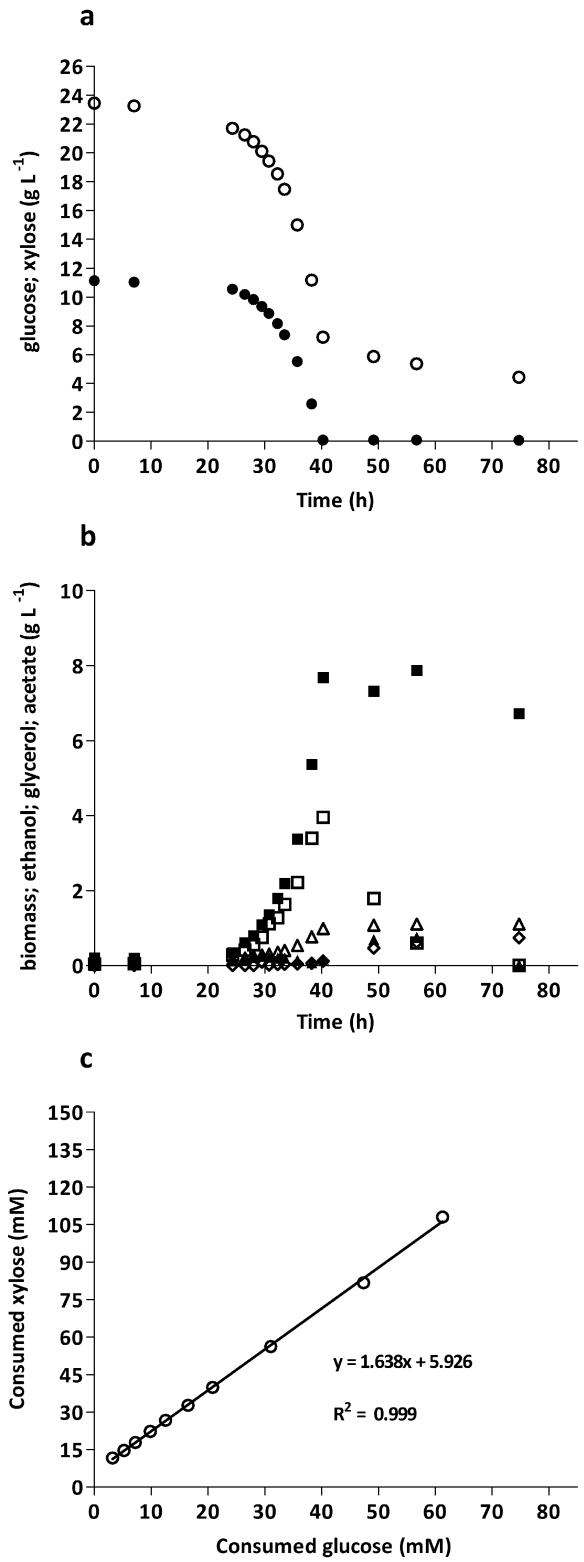

Figure 3. Sugar consumption, biomass and metabolite production profiles of the evolved *S. cerevisiae* strain IMS0629 (*pgi1*Δ *rpe1*Δ *gnd1*Δ *gnd2*Δ *gndA xylA XKS1*↑ PPP↑), grown on SM with 10 g L^{-1} glucose and 20 g L^{-1} xylose in aerobic bioreactor batch cultures (pH 5, 30°C). Cultures were grown in duplicate; the data shown are from a single representative culture. **a**: filled circles glucose, open circles xylose; **b**: filled squares biomass, open squares ethanol, filled triangles acetate, open triangles glycerol, open diamonds xylitol; **c**: ratio of xylose and glucose consumption during exponential growth phase.

Table 2. Product yields, biomass-specific sugar uptake and production rates in aerobic bioreactor batch cultures of evolved strain *S. cerevisiae* IMS0629 (*pgi1*Δ *rpe1*Δ *gnd1*Δ *gnd2*Δ *gndA xylA XKS1*↑ PPP↑) on SM supplemented with 10 g L^{-1} glucose and 20 g L^{-1} xylose (pH 5, 30°C).

Growth rate (h^{-1})	0.18 ± 0.00
Glucose-xylose consumption ratio mol mol^{-1}	1.64 ± 0.00
Spec. xylose uptake rate mmol (g biomass)$^{-1}$ h^{-1}	2.52 ± 0.00
Spec. glucose uptake rate mmol (g biomass)$^{-1}$ h^{-1}	1.54 ± 0.07
Spec. glycerol production rate mmol (g biomass)$^{-1}$ h^{-1}	0.23 ± 0.01
Spec. ethanol production rate mmol (g biomass)$^{-1}$ h^{-1}	2.25 ± 0.37
Spec. CO_2 production rate mmol (g biomass)$^{-1}$ h^{-1}	10.43 ± 0.98
Spec. O_2 uptake rate mmol (g biomass)$^{-1}$ h^{-1}	6.87 ± 0.56
Respiratory quotient	1.52 ± 0.03
Biomass yield g biomass (g sugars)$^{-1}$	0.28 ± 0.00
Ethanol yield g (g sugars)$^{-1}$	0.18 ± 0.00

Biomass-specific rates, yields and ratios were calculated from samples taken during the mid-exponential growth phase and represent averages ± mean deviation of independent duplicate cultures. Ethanol yield was corrected for evaporation.

Mutations in *HXK2*, *RSP5* and *GAL83* stimulate co-consumption of xylose and glucose in aerobic cultures of xylose-consuming *S. cerevisiae*

To investigate whether mutations acquired during evolution for forced co-consumption of glucose and xylose were relevant for mixed-sugar utilisation in a strain without forced glucose-xylose co-consumption, we focused on mutations in *HXK2* and *RSP5* (which were present in both IMS0629 and IMS0634) and/or *GAL83*. Mutations in these genes were introduced into an engineered, non-evolved xylose-consuming *S. cerevisiae* strain background (IMX994, Table 1). Overexpression of *xylA* was accomplished by transforming strains with the multicopy *xylA* expression vector pAKX002 (Kuyper *et al.* 2003). In aerobic shake-flask cultures grown on 10 g L^{-1} glucose and 10 g L^{-1} xylose, the reference strain IMU079 (*XKS1*↑ PPP↑ pAKX002) displayed a pronounced biphasic growth profile and only a minor co-consumption of the two sugars (0.13 mol xylose (mol glucose)$^{-1}$; Table 4, Fig. 4, Additional File 9). Co-consumption was strongly enhanced in the congenic *hxk2*Δ strain IMX1485, which showed a 3-fold higher molar ratio of xylose and glucose consumption (0.41 mol mol^{-1}). However, its specific growth rate before glucose depletion (0.28 h^{-1}) was 13% lower than that of the reference strain (Table 4). Strain IMX1487 (*rsp5*Δ), which showed a 20% lower specific growth rate than the reference strain, showed a slight improvement in co-consumption (Table 4). Deletion of *GAL83* (strain IMX1486) affected neither sugar co-consumption nor growth rate. In contrast, replacement of *GAL83* by $GAL83^{G673T}$ (strain IMX1488) resulted in a 40% higher co-consumption of glucose and xylose than observed in the reference strain IMU079, without affecting growth rate (Table 4).

Since independently evolved glucose-xylose co-consuming strains contained putative loss-of-function mutations in *HXK2* and *RSP5*, both genes were deleted in strain IMX1515 (*hxk2*Δ *rsp5*Δ *XKS1*↑ PPP↑ pAKX002). Similarly, deletion of *HXK2* and introduction of $GAL83^{G673T}$ were combined in strain IMX1583 (*hxk2*Δ *gal83*::$GAL83^{G673T}$ *XKS1*↑ PPP↑ pAKX002). Co-consumption ratios in the two strains (0.60 and 0.49 mol xylose (mol glucose)$^{-1}$, respectively) were 4- to 5-fold higher than in the reference strain IMU079 (Table 4, Fig. 4, Additional File 9). However, strain IMX1515 exhibited a 40% lower specific growth rate (0.19 h^{-1}) than the reference strain, resulting in a 9 h

Table 3. Mutations identified by whole-genome sequencing of glucose-xylose co-consuming *S. cerevisiae* strains evolved for fast growth at high glucose concentrations.

Strain and gene	Nucleotide change	Amino acid change	Description
IMS0629			
CYC8	G896A	W299 →Stop	General transcriptional co-repressor; acts together with Tup1; also acts as part of a transcriptional co-activator complex that recruits the SWI/SNF and SAGA complexes to promoters; can form the prion [OCT+]
GAL83	G673T	D225Y	One of three possible beta-subunits of the Snf1 kinase complex; allows nuclear localisation of the Snf1 kinase complex in the presence of a non-fermentable carbon source
RSP5	G686A	G229D	NEDD4 family E3 ubiquitin ligase; regulates processes including MVB sorting, the heat shock response, transcription, endocytosis and ribosome stability; ubiquitinates Sec23, Sna3, Ste4, Nfi1, Rpo21 and Sem1; autoubiquitinates; deubiquitinated by Ubp2; regulated by SUMO ligase Siz1, in turn regulates Siz1p SUMO ligase activity; required for efficient Golgi-to-ER trafficking in COPI mutants
HXK2	C927G	Y309 →Stop	Hexokinase isoenzyme 2; phosphorylates glucose in cytosol; predominant hexokinase during growth on glucose; represses expression of *HXK1*, *GLK1*
RBH1	C190A	Q64K	Putative protein of unknown function; expression is cell-cycle regulated as shown by microarray analysis; potential regulatory target of Mbp1, which binds to the YJL181W promoter region; contains a PH-like domain
DCS1	C636G	Y212→Stop	Non-essential hydrolase involved in mRNA decapping; activates Xrn1; may function in a feedback mechanism to regulate deadenylation, contains pyrophosphatase activity and a HIT (histidine triad) motif; acts as inhibitor of neutral trehalase Nth1; required for growth on glycerol medium
IMS0634			
RSP5	Internal deletion (41 nucleotides)	Frameshift	NEDD4 family E3 ubiquitin ligase; regulates processes including: MVB sorting, the heat shock response, transcription, endocytosis and ribosome stability; ubiquitinates Sec23, Sna3, Ste4, Nfi1, Rpo21 and Sem1; autoubiquitinates; deubiquitinated by Ubp2; regulated by SUMO ligase Siz1, in turn regulates Siz1p SUMO ligase activity; required for efficient Golgi-to-ER trafficking in COPI mutants
HXK2	G1027C	D343H	Hexokinase isoenzyme 2; phosphorylates glucose in cytosol; predominant hexokinase during growth on glucose; represses expression of *HXK1*, *GLK1*

Gene descriptions were taken from the *Saccharomyces* Genome Database (https://www.yeastgenome.org/, Accessed 14 December 2017).

Table 4. Specific growth rates (μ) and ratio of xylose and glucose consumption in aerobic shake-flask cultures of strains IMU079 (*XKS1*↑ PPP↑ pAKX002), IMX1485 (*hkx2*Δ *XKS1*↑ PPP↑ pAKX002), IMX1486 (*gal83*Δ *XKS1*↑ PPP↑ pAKX002), IMX1487 (*rsp5*Δ *XKS1*↑ PPP↑ pAKX002), IMX1488 (*gal83*::*GAL83*^{G673T} *XKS1*↑ PPP↑ pAKX002), IMX1515 (*hxk2*Δ *rsp5*Δ *XKS1*↑ PPP↑ pAKX002) and IMX1583 (*hxk2*Δ *gal83*::*GAL83*^{G673T} *XKS1*↑ PPP↑ pAKX002) grown on SM (urea as nitrogen source) with 10 g L^{-1} glucose and 10 g L^{-1} xylose (pH 6, 30°C).

Strain	Relevant genotype	μ (h^{-1})	Xylose-glucose consumption ratio (mol mol^{-1})
IMU079	*HXK2 RSP5 GAL83*	0.32 ± 0.01	0.13 ± 0.00
IMX1485	*hxk2*Δ	0.28 ± 0.00	0.41 ± 0.01
IMX1486	*gal83*Δ	0.31 ± 0.00	0.14 ± 0.01
IMX1487	*rsp5*Δ	0.26 ± 0.00	0.15 ± 0.00
IMX1488	*gal83*::*GAL83*^{G673T}	0.31 ± 0.00	0.18 ± 0.01
IMX1515	*hxk2*Δ *rsp5*Δ	0.19 ± 0.00	0.60 ± 0.00
IMX1583	*hxk2*Δ *gal83*::*GAL83*^{G673T}	0.31 ± 0.00	0.49 ± 0.00

Growth rates and ratios were calculated from samples taken during the mid-exponential growth phase and represent averages ± mean deviation of independent duplicate cultures.

extension of the fermentation experiments (Fig. 4, Additional File 9). In contrast, strain IMX1583 combined a high co-consumption ratio with the same specific growth rate as that of the reference strain.

Combined mutations in *HXK2* and *GAL83* significantly accelerate conversion of glucose-xylose mixtures by anaerobic cultures of xylose-consuming *S. cerevisiae*

To investigate the impact of the identified mutations under more industrially relevant conditions, anaerobic growth of the reference xylose-fermenting strain IMU079 (*XKS1*↑ PPP↑ pAKX002) in bioreactor batch experiments was compared with that of the two congenic double mutants IMX1515 (*hxk2*Δ *rsp5*Δ) and IMX1583 (*hxk2*Δ *gal83*::GAL83^{G673T}) that showed the highest glucose-xylose co-consumption in the aerobic shake-flask experiments. The anaerobic cultures were grown on 20 g L^{-1} glucose and 10 g L^{-1} xylose to simulate the relative concentrations of these sugars typically found in corn stover and wheat straw hydrolysates (van Maris *et al.* 2006).

In the anaerobic batch cultures, strains IMU079, IMX1515 and IMX1583 all produced CO_2, biomass, ethanol and glycerol as main products, with a minor production of acetate (Table 5, Fig. 5, Additional File 10). The strains did not produce xylitol during exponential growth and low concentrations of xylitol in cultures of strain IMU079 (2.2 ± 0.1 mmol L^{-1}) were only observed at the end of fermentation. As observed in aerobic cultures (Fig. 4), strain IMU079 showed a clear biphasic growth profile in the anaerobic bioreactors (Fig. 5, Additional File 10), during which a fast glucose phase (ca. 16 h) was followed by a much slower and decelerating xylose consumption phase. During the glucose phase, this reference strain maintained a specific growth rate of 0.29 h^{-1} and a glucose-xylose co-consumption ratio of 0.14 mol mol^{-1} (Table 5). After a ca. 30-h lag phase (Fig. 5, Additional

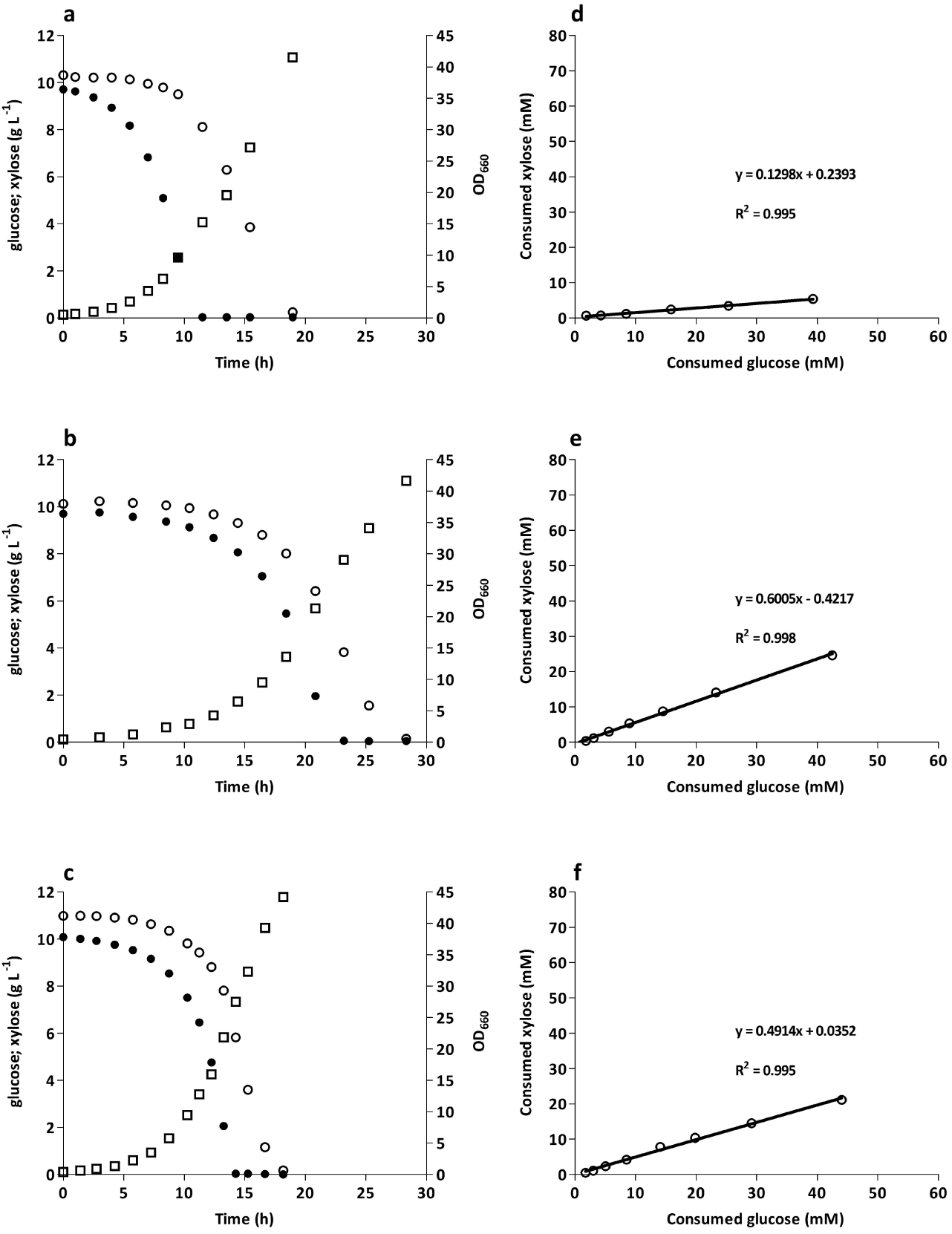

Figure 4. Consumption of glucose and xylose and growth of strains IMU079 (*XKS1*↑ PPP↑ pAKX002; a, d), IMX1515 (*hxk2*Δ *rsp5*Δ *XKS1*↑ PPP↑ pAKX002; b, e) and IMX1583 (*hxk2*Δ *gal83::GAL83*^{G673T} *XKS1*↑ PPP↑ pAKX002; c, f) in batch cultures. The three strains were grown on SM (urea as nitrogen source) with 10 g L^{-1} glucose and 10 g L^{-1} xylose in aerobic shake-flask cultures (pH 6, 30°C). a, b, c: filled circles glucose, open circles xylose, open squares OD_{660}; d, e, f: ratio of xylose and glucose consumption during exponential growth phase. Data for independent duplicate cultures are provided in Additional File 9.

Table 5. Product yields, biomass-specific rates and sugar uptake ratios in anaerobic bioreactor batch cultures of strains IMU079 (*XKS1*↑ PPP↑ pAKX002), IMX1515 (*hxk2*Δ *rsp5*Δ *XKS1*↑ PPP↑ pAKX002) and IMX1583 (*hxk2*Δ *gal83*::*GAL83*^{G673T} *XKS1*↑ PPP↑ pAKX002) grown on SM supplemented with 20 g L^{-1} glucose and 10 g L^{-1} xylose (pH 5, 30°C).

Strain	IMU079	IMX1515	IMX1583
Relevant genotype	*HXK2 RSP5 GAL83*	*hxk2*Δ *rsp5*Δ	*hxk2*Δ *gal83*::*GAL83*^{G673T}
μ (h^{-1})	0.29 ± 0.01	0.07 ± 0.00	0.21 ± 0.00
Spec. xylose uptake rate mmol (g biomass)$^{-1}$ h^{-1}	2.22 ± 0.14	2.50 ± 0.12	3.19 ± 0.02
Spec. glucose uptake rate mmol (g biomass)$^{-1}$ h^{-1}	15.65 ± 0.52	5.58 ± 0.08	10.09 ± 0.08
Glucose-xylose consumption ratio (mol mol^{-1})	0.14 ± 0.00	0.45 ± 0.03	0.32 ± 0.01
Biomass yield on sugars (g biomass g^{-1})	0.09 ± 0.01	0.05 ± 0.00	0.09 ± 0.00
Ethanol yield on sugars (g g^{-1})	0.37 ± 0.00	0.43 ± 0.00	0.38 ± 0.01
Glycerol yield on sugars (g g^{-1})	0.10 ± 0.00	0.06 ± 0.00	0.08 ± 0.00
Ratio glycerol production on biomass production (mmol (g biomass)$^{-1}$)	11.5 ± 0.60	12.0 ± 0.50	9.9 ± 0.10
Xylitol production (mmol L^{-1})	2.22 ± 0.06	0.90 ± 0.04	0.35 ± 0.04

Rates, yields and ratios were calculated from samples taken during the mid-exponential growth phase and represent averages ± mean deviation of independent duplicate cultures. Ethanol yields were corrected for evaporation.

File 10), strain IMX1515 exhibited an exponential growth rate of 0.07 ± 0.00 h^{-1}, with a high glucose-xylose co-consumption ratio (0.45 ± 0.03 mol mol^{-1}). Mainly as a result of its lag phase, strain IMX1515 took longer to consume all sugars than the reference strain IMU079, but its xylose-consumption phase was ca. 65% shorter (ca. 14 and 43 h, respectively; Fig. 5, Additional File 10).

In contrast to strain IMX1515, strain IMX1583 (*hxk2*Δ *gal83*::*GAL83*^{G673T} *XKS1*↑ PPP↑ pAKX002) did not exhibit a lag phase but immediately started exponential growth at 0.21 h^{-1} (Fig. 5). A comparison of biomass-specific uptake rates of xylose and glucose in the anaerobic batch experiments showed that strain IMX1583 maintained a 44% higher xylose uptake rate than strain IMU079 before glucose exhaustion (Table 5). Moreover, both strains IMX1515 and IMX1583 did not show the pronounced decline of xylose consumption after glucose exhaustion that was observed in the reference strain (Fig. 5, Additional File 10). As a result, the xylose consumption phase in anaerobic cultures of strain IMX1583 was 80% shorter than that strain IMU079 (ca. 9 h compared to 43 h), thereby reducing the time required for complete sugar conversion by over 24 h (Fig. 5).

DISCUSSION

Engineering *S. cerevisiae* for forced co-consumption of xylose and glucose

The key objective of this study was to develop and test a strain platform that, via laboratory evolution and subsequent genome resequencing, can be used to identify mutations that support co-metabolism of xylose and glucose. In previous studies, laboratory evolution of glucose-phosphorylation-negative, pentose-fermenting strains in the presence of glucose yielded valuable leads for improving utilisation of glucose-xylose mixtures, including mutations in *HXT* genes that improved pentose uptake in the presence of glucose (Farwick *et al.* 2014; Nijland *et al.* 2014, 2017; Wisselink, Van Maris and Pronk 2015). The strategy described in this study differs from these previous studies as it not only enabled selection for xylose utilisation in the presence of glucose, but also for simultaneous metabolism of the two sugars. The molar ratio of xylose and glucose co-consumption (1.64 mol xylose (mol glucose)$^{-1}$) by the evolved strain IMS0629 is the highest reported to date for batch cultures of *S. cerevisiae* (Katahira *et al.* 2008; Shen *et al.* 2012, 2015; Gonçalves *et al.* 2014; Nijland *et al.* 2014; Westman *et al.* 2014; Shin *et al.* 2015).

Inactivation of *PGI1* played a key role in forcing simultaneous utilisation of xylose and glucose (Fig. 1). To pre-empt the well-documented inability of *S. cerevisiae pgi1*Δ mutants to reoxidise the NADPH that is generated when metabolism of glucose-6-phosphate is rerouted through the oxidative PPP (Boles, Lehnert and Zimmermann 1993; Heux, Cadiere and Dequin 2008), we replaced Gnd1 and Gnd2 with the NAD^+-linked bacterial 6-phosphogluconate dehydrogenase GndA (Papapetridis *et al.* 2016). Together with the co-consumption of xylose, via an engineered pathway that did not involve NAD(P)H generation (Fig. 1), these modifications enabled the engineered strain IMX1046 to grow on mixtures of xylose and 1 g L^{-1} glucose, without the fructose supplementation that is normally required for growth of *pgi1*-null mutants on glucose (Aguilera 1986; Boles, Lehnert and Zimmermann 1993). The evolved strain IMS0629 consumed 8.6 mmol glucose (g biomass)$^{-1}$ in aerobic batch cultures (Table 2), which is close to the requirement of 9.3 mmol NADPH (g biomass)$^{-1}$ for aerobic growth on glucose of wild-type *S. cerevisiae* (Bruinenberg, Van Dijken and Scheffers 1983). However, since glucose-6-phosphate is a key biosynthetic precursor, not all glucose consumed by the cultures can be converted through the oxidative PPP. Additional enzymes such as $NADP^+$-dependent acetaldehyde dehydrogenase Ald6 (Grabowska and Chelstowska 2003; Celton *et al.* 2012; Papapetridis *et al.* 2016) are therefore likely to have supplemented NADPH generation via the oxidative PPP in the 'forced co-consumption' strains.

Improvement of mixed-sugar fermentation in aerobic and anaerobic cultures of xylose-fermenting *S. cerevisiae*

Mutations in *HXK2*, *RSP5* and *GAL83* were reverse engineered into a non-evolved strain (*XKS1*↑ PPP↑) to investigate whether mutations acquired during evolution of strain IMX1046 (*pgi1*Δ *rpe1*Δ *gnd1*Δ *gnd2*Δ *gndA xylA XKS1*↑ PPP↑) on glucose-xylose mixtures would also stimulate mixed-substrate utilisation in a genetic background that does not impose forced co-utilisation. During growth on glucose-xylose mixtures, the reference strain IMU079 (*XKS1*↑ PPP↑ pAKX002) displayed the typical biphasic growth profile seen in non-evolved, xylose-consuming strains that express a basic, functional xylose-isomerase (XI)-based xylose fermentation pathway (Kuyper *et al.* 2003, 2005a). Biphasic growth was especially pronounced in anaerobic cultures,

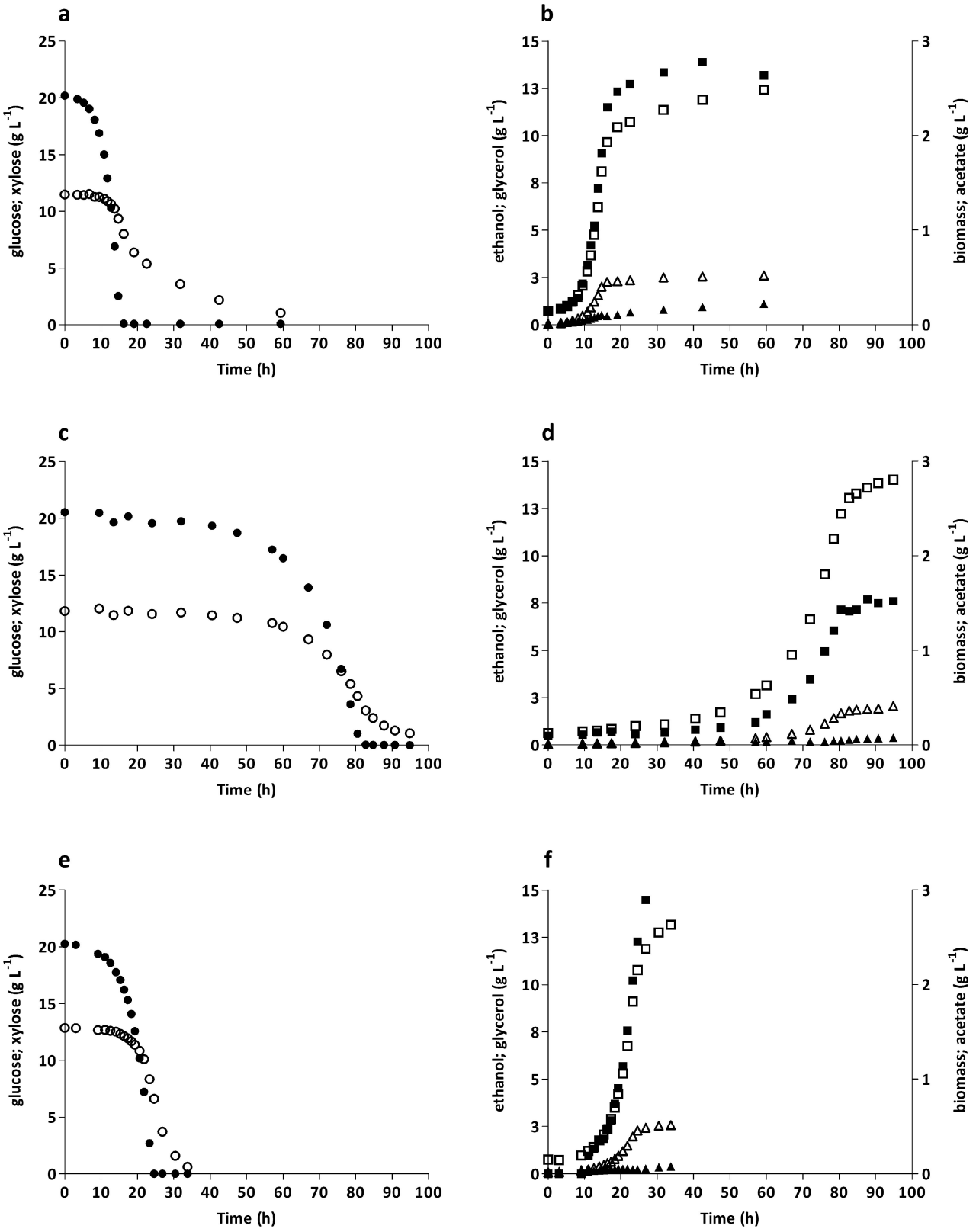

Figure 5. Sugar consumption, biomass and metabolite production profiles of *S. cerevisiae* strains IMU079 (XKS1↑ PPP↑ pAKX002; a, b), IMX1515 (*hxk2*Δ *rsp5*Δ XKS1↑ PPP↑ pAKX002; c, d) and IMX1583 (*hxk2*Δ *gal83*::*GAL83*^{G673T} XKS1↑ PPP↑ pAKX002; e, f), grown on SM with 20 g L^{-1} glucose and 10 g L^{-1} xylose in anaerobic bioreactor batch cultures (pH 5, 30°C). Cultures were grown in duplicate, the data shown are from a single representative culture. a, c, e: filled circles glucose, open circles xylose; b, d, f: filled squares biomass, open squares ethanol, filled triangles acetate, open triangles glycerol. Data on ethanol corrected for evaporation. For duplicate cultures, refer to Additional File 10.

in which the xylose consumption rate collapsed upon glucose depletion (Fig. 5). Deletion of *HXK2*, either combined with the deletion of *RSP5* or with the introduction of a *GAL83*^{G673T} mutation, strongly improved mixed-sugar fermentation kinetics, both by increased co-utilisation and by faster conversion of xylose after glucose had been depleted (Figs 4 and 5).

Hxk2, the major hexokinase in *S. cerevisiae*, plays an additional key role in transcriptional repression of a large set of yeast genes (Entian 1980; Entian and Fröhlich 1984; Peláez, Herrero and Moreno 2010) by glucose. Deletion of *HXK2* has been shown to enhance co-consumption of combinations of natural substrates (glucose-galactose, glucose-sucrose and glucose-ethanol) in batch cultures (Raamsdonk *et al.* 2001). During exponential growth on glucose in batch cultures, *hxk2*Δ mutants show increased transcription of the high-affinity hexose transporter genes *HXT2* and *HXT7* and decreased transcription of the low-affinity hexose transporter genes *HXT1* and *HXT3* (Petit *et al.* 2000). The high-affinity Hxt transporters, which in wild-type strains are only expressed at low glucose concentrations (Diderich *et al.* 1999), have a much lower K_m for xylose than their low-affinity counterparts (Hamacher *et al.* 2002; Lee *et al.* 2002). Several studies have demonstrated that overexpression of high-affinity hexose transporters stimulates xylose uptake (Subtil and Boles 2012; Farwick *et al.* 2014; Gonçalves *et al.* 2014; Nijland *et al.* 2014, 2016; Reznicek *et al.* 2015; Shin *et al.* 2015; Jansen *et al.* 2017). The observed improved co-utilisation of glucose and xylose upon inactivation of *HXK2* may therefore reflect an increased abundance of high-affinity hexose transporters in the yeast plasma membrane during growth on glucose-xylose mixtures. A recent *in silico* study identified *HXK2* as potential target for improving xylose uptake rates in *S. cerevisiae* (Miskovic *et al.* 2017). However, subsequent deletion of *HXK2* in a strain expressing a XR/XDH-based pathway resulted in faster xylose uptake but also increased by-product formation and reduced ethanol productivity (Miskovic *et al.* 2017). The absence of such negative effects in the present study is in line with reports that XI-based strains are less prone to by-product formation than XR/XDH-based strains (Moysés *et al.* 2016; Jansen *et al.* 2017).

Rsp5, the only representative of the NEDD4 family of E3-ubiquitin ligases in *S. cerevisiae*, is involved in regulation of a multitude of cellular processes, including intracellular protein trafficking, regulation of the large subunit of RNA polymerase II, ribosome stability, regulation of fatty acid synthesis and stress response (Huibregtse, Yang and Beaudenon 1997; Belgareh-Touzé *et al.* 2008; Kaliszewski and Zoładek 2008; Shcherbik and Pestov 2011). This multitude of roles may explain the reduced growth rate of the *rsp5*Δ strains (Tables 4 and 5) in this study. Involvement of Rsp5 in ubiquitination and subsequent endocytosis of the high-affinity hexose transporters Hxt6 and Hxt7 (Krampe *et al.* 1998; Haguenauer-Tsapis and André 2004) could explain the strong synergistic effect of the *hxk2*Δ and *rsp5*Δ deletions: while deletion of *HXK2* prevents glucose repression of the synthesis of these transporters, deletion of *RSP5* could prevent their ubiquitination and removal from the membrane. Removal of ubiquitination sites in the hexose transporters Hxt1 and Hxt36 was previously shown to enhance xylose uptake by *S. cerevisiae* (Nijland *et al.* 2016). Our results suggest that a similar modification of Hxt6 and Hxt7 could also be beneficial.

Gal83 is one of three possible β-subunits of the Snf1-kinase complex, which enables transcription of glucose-repressed genes at low glucose concentrations (for reviews, see Gancedo 1998; Schüller 2003). At non-repressing glucose concentrations, Gal83 directs the Snf1-Gal83 complex to the cell nucleus (Vincent *et al.* 2001), where it mediates transcriptional upregulation of genes involved in utilisation of alternative carbon sources (Vincent and Carlson 1999). Targets of the Snf1-Gal83 complex include the *GAL* regulon (Matsumoto, Toh-e and Oshima 1981; Erickson and Johnston 1993) and the high-affinity hexose transporter genes *HXT2* and *HXT4* (Özcan and Johnston 1999). The D225Y substitution, which stimulated glucose-xylose co-consumption in the present study, is located in the glycogen-binding domain of Gal83 (residues 161–243; Momcilovic *et al.* 2008). Other mutations in this domain have been shown to cause transcription of Snf1-Gal83 targets in the presence of glucose (Wiatrowski *et al.* 2004; Momcilovic *et al.* 2008; Mangat *et al.* 2010). In contrast to deletion of the transcriptional regulator *CYC8* (Nijland *et al.* 2017), which also stimulated co-utilisation but caused severe reductions of the specific growth rate of engineered strains, the *GAL83*^{G673T} mutation did not have a strong impact on growth rate (Tables 4 and 5). The synergistic effect of the *hxk2*Δ and *GAL83*^{G673T} mutations may be related to the involvement of Hxk2 in deactivation of Snf1 in the presence of glucose, causing constitutive activity of the Snf1-Gal83 complex in *hxk2*-null mutants (Gancedo 1998; Schüller 2003).

The reverse engineered mutations in *HXK2* and *GAL83* or *RSP5* not only stimulated simultaneous utilisation of xylose and glucose when both sugars were present, but also prevented the sharp decline in xylose uptake rates that occurred in the reference strain IMU079 (*XKS1*↑ PPP↑ pAKX002). In the reference strain, the biomass-specific rate of xylose consumption, probably mediated by low- or moderate-affinity Hxt transporters, declined to values below 0.5 mmol (g biomass)$^{-1}$ h^{-1} after glucose depletion (Fig. 5, Additional File 10). Under anaerobic conditions, this low rate of xylose fermentation would correspond to a biomass-specific rate of ATP production of 0.8 mmol (g biomass)$^{-1}$ h^{-1}. This value is lower than the estimated ATP requirement for cellular maintenance of *S. cerevisiae* (ca. 1 mmol ATP (g biomass)$^{-1}$ h^{-1}; Boender *et al.* 2009). Since protein synthesis is a highly ATP-intensive process (Canelas *et al.* 2010), an inability of the reference strain to functionally express high-affinity hexose transporters upon glucose depletion may therefore reflect an energy shortage. A similar effect was observed during transitions between glucose and galactose growth in anaerobic *S. cerevisiae* cultures (van den Brink *et al.* 2009). By already expressing functional high-affinity transporters before glucose was depleted, the *hxk2*Δ *rsp5*Δ and *hxk2*Δ *GAL83*^{G673T} genotypes may have enabled cells to avoid such a bioenergetic 'valley of death' upon the transition to xylose fermentation. In industrial processes using lignocellulosic feedstocks, this energetic challenge is likely to be even more stringent due to the presence of compounds such as acetic acid that increase maintenance energy requirements (Verduyn *et al.* 1992; Abbott *et al.* 2007; Bellissimi *et al.* 2009).

While reverse engineering of *HXK2*, *RSP5* and *GAL83* mutations demonstrated the relevance of the forced co-utilisation strategy demonstrated in this study, they do not exhaust its possibilities. Prolongation of the evolution experiments, combined with anaerobic conditions and/or a further increase of the glucose to xylose ratio in the medium, may allow for selection of additional relevant mutations. The IMS0629 strain may also be used to select mutations that enable efficient co-utilisation of glucose and xylose at different concentrations or in lignocellulosic hydrolysates that, in addition to fermentable sugars, contain inhibitors of yeast performance (Palmqvist and Hahn-Hägerdal 2000; Klinke *et al.* 2002; Almeida *et al.* 2007). Alternatively, the strain design can be adapted to enable selection for co-metabolism of other sugars, for example by

replacing the xylose pathway by a bacterial pathway for conversion of L-arabinose into xylulose-5-phosphate (Becker and Boles 2003; Wisselink *et al.* 2007). This strategy can be extended to optimising the yeast metabolic network for aerobic production of economically relevant compounds other than ethanol from lignocellulosic hydrolysates. In particular, imposing fixed stoichiometries of glycolytic and (non-oxidative) PPP reactions may offer interesting options for high-yield production of compounds whose synthesis requires a large net input of PPP intermediates and/or NADPH, such as aromatic compounds and lipids (Tehlivets, Scheuringer and Kohlwein 2007; Klug and Daum 2014; Gottardi *et al.* 2017).

CONCLUSIONS

Engineering of carbon and redox metabolism yielded an *S. cerevisiae* strain whose growth was strictly dependent on the simultaneous uptake and metabolism of xylose and glucose. Laboratory evolution improved growth of the resulting strains on mixtures of xylose and glucose at elevated glucose concentrations. Mutations in *HXK2*, *RSP5* and *GAL83* were identified by genome sequencing of the evolved strains. Upon their combined introduction into an engineered xylose-fermenting yeast strain, these mutations strongly stimulated simultaneous utilisation of xylose and glucose and, after depletion of glucose, fast conversion of the remaining xylose. The developed strain platform and modified versions thereof can be used for identification of further metabolic engineering targets for improving the performance of yeast strains in industrial processes based on lignocellulosic feedstocks.

SUPPLEMENTARY DATA

Supplementary data are available at *FEMSYR* online.

ACKNOWLEDGEMENTS

We thank Jasmine Bracher and Oscar Martinez for construction of strain IMU079. We thank Jean-Marc Daran and Pilar de la Torre for advice on molecular biology, Marcel van den Broek for assistance with bioinformatics analyses and Erik de Hulster for advice on fermentations. We thank Laura Valk for stimulating discussions.

Availability of supporting data

The genomic sequence of strains IMS0629 and IMS0634 have been deposited in Genbank (http://www.ncbi.nlm.nih.gov/), BioProject number PRJNA433919.

Author's contributions

IP, MDV, AJAvM and JTP designed experiments. IP, MDV and JTP wrote the first draft of the manuscript. IP and MDV constructed yeast strains and performed fermentations. SJW constructed yeast strains and performed *in silico* analyses. MG designed and carried out fermentations. All authors read and commented upon the draft manuscript and approved the final version.

Funding

The PhD project of IP is funded by DSM. This work was performed within the BE-Basic R&D Program (http://www.be-basic.org/), which is financially supported by an EOS Long Term grant from the Dutch Ministry of Economic Affairs, Agriculture and Innovation (EL&I).

Competing interests

IP, MDV, AJAvM and JTP are co-inventors on a patent application related to the content of this work.

REFERENCES

Abbott DA, Knijnenburg TA, De Poorter LMI *et al.* Generic and specific transcriptional responses to different weak organic acids in anaerobic chemostat cultures of *Saccharomyces cerevisiae*. *FEMS Yeast Res* 2007;**7**:819–33.

Aguilera A. Deletion of the phosphoglucose isomerase structural gene makes growth and sporulation glucose dependent in *Saccharomyces cerevisiae*. *Mol Gen Genet* 1986;**204**:310–6.

Almeida JRM, Modig T, Petersson A *et al.* Increased tolerance and conversion of inhibitors in lignocellulosic hydrolysates by *Saccharomyces cerevisiae*. *J Chem Technol Biot* 2007;**82**:340–9.

Alper H, Stephanopoulos G. Engineering for biofuels: exploiting innate microbial capacity or importing biosynthetic potential? *Nat Rev Microbiol* 2009;**7**:715–23.

Ask M, Bettiga M, Duraiswamy VR *et al.* Pulsed addition of HMF and furfural to batch-grown xylose-utilizing *Saccharomyces cerevisiae* results in different physiological responses in glucose and xylose consumption phase. *Biotechnol Biofuels* 2013;**6**:181.

Aung HW, Henry SA, Walker LP. Revising the representation of fatty acid, glycerolipid, and glycerophospholipid metabolism in the consensus model of yeast metabolism. *Ind Biotechnol* 2013;**9**:215–28.

Bakker BM, Overkamp KM, van Maris AJA *et al.* Stoichiometry and compartmentation of NADH metabolism in *Saccharomyces cerevisiae*. *FEMS Microbiol Rev* 2001;**25**:15–37.

Basso LC, Basso T, Nitsche Rocha S. Ethanol production in Brazil: the industrial process and its impact on yeast fermentation. *Biofuel Production - Recent Developments and Prospects*. Rijeka: IntechOpen, 2011, DOI: 10.5772/17047.

Becker J, Boles E. A modified *Saccharomyces cerevisiae* strain that consumes l-arabinose and produces ethanol. *Appl Environ Microb* 2003;**69**:4144–50.

Becker SA, Feist AM, Mo ML *et al.* Quantitative prediction of cellular metabolism with constraint-based models: the COBRA Toolbox. *Nat Protoc* 2007;**2**:727–38.

Belgareh-Touzé N, Léon S, Erpapazoglou Z *et al.* Versatile role of the yeast ubiquitin ligase Rsp5p in intracellular trafficking: Figure 1. *Biochem Soc Trans* 2008;**36**:791–6.

Bellissimi E, Van Dijken JP, Pronk JT *et al.* Effects of acetic acid on the kinetics of xylose fermentation by an engineered, xylose-isomerase-based *Saccharomyces cerevisiae* strain. *FEMS Yeast Res* 2009;**9**:358–64.

Boender LGM, de Hulster EAF, van Maris AJA *et al.* Quantitative physiology of *Saccharomyces cerevisiae* at near-zero specific growth rates. *Appl Environ Microb* 2009;**75**:5607–14.

Boles E, Lehnert W, Zimmermann FK. The role of the NAD-dependent glutamate dehydrogenase in restoring growth on glucose of a *Saccharomyces cerevisiae* phosphoglucose isomerase mutant. *Eur J Biochem* 1993;**217**:469–77.

Bruinenberg PM, Van Dijken JP, Scheffers WA. A theoretical analysis of NADPH production and consumption in yeasts. *Microbiology* 1983;**129**:953–64.

Canelas AB, Harrison N, Fazio A *et al.* Integrated multilaboratory systems biology reveals differences in protein metabolism between two reference yeast strains. *Nat Commun* 2010;**1**:145.

Celton M, Sanchez I, Goelzer A *et al.* A comparative transcriptomic, fluxomic and metabolomic analysis of the response of *Saccharomyces cerevisiae* to increases in NADPH oxidation. *BMC Genomics* 2012;**13**:317.

De Winde JH, Crauwels M, Hohmann S *et al.* Differential requirement of the yeast sugar kinases for sugar sensing in establishing the catabolite-repressed state. *Eur J Biochem* 1996;**241**:633–43.

DiCarlo JE, Norville JE, Mali P *et al.* Genome engineering in *Saccharomyces cerevisiae* using CRISPR-Cas systems. *Nucleic Acids Res* 2013;**41**:4336–43.

Dickinson JR, Sobanski MA, Hewlins MJE. In *Saccharomyces cerevisiae* deletion of phosphoglucose isomerase can be suppressed by increased activities of enzymes of the hexose monophosphate pathway. *Microbiology* 1995;**141**: 385–91.

Diderich JA, Schepper M, van Hoek P *et al.* Glucose uptake kinetics and transcription of *HXT*Genes in chemostat cultures of *Saccharomyces cerevisiae*. *J Biol Chem* 1999;**274**:15350–9.

Entian K-D. Genetic and biochemical evidence for hexokinase PII as a key enzyme involved in carbon catabolite repression in yeast. *Mol Gen Genet* 1980;**178**:633–7.

Entian K-D, Fröhlich K-U. *Saccharomyces cerevisiae* mutants provide evidence of hexokinase PII as a bifunctional enzyme with catalytic and regulatory domains for triggering catabolite repression. *J Bacteriol* 1984;**158**:29–35.

Entian K-D, Kötter P. 25 yeast genetic strain and plasmid collections. In: Stansfield I, Stark MJR (eds.) *Methods in Microbiology*, vol. 36. London: Academic Press, 2007, 629–66.

Erickson JR, Johnston M. Genetic and molecular characterization of Gal83: Its interaction and similarities with other genes involved in glucose repression in *Saccharomyces cerevisiae*. *Genetics* 1993;**135**:655–64.

Farwick A, Bruder S, Schadeweg V *et al.* Engineering of yeast hexose transporters to transport D-xylose without inhibition by D-glucose. *Proc Natl Acad Sci USA* 2014;**111**:5159–64.

Fulton LM, Lynd LR, Körner A *et al.* The need for biofuels as part of a low carbon energy future. *Biofuels Bioprod Bioref* 2015;**9**:476–83.

Gancedo JM. Yeast carbon catabolite repression. *Microbiol Mol Biol R* 1998;**62**:334–61.

Garcia Sanchez R, Karhumaa K, Fonseca C *et al.* Improved xylose and arabinose utilization by an industrial recombinant *Saccharomyces cerevisiae* strain using evolutionary engineering. *Biotechnol Biofuels* 2010;**3**:13.

Gawand P, Hyland P, Ekins A *et al.* Novel approach to engineer strains for simultaneous sugar utilization. *Metab Eng* 2013;**20**:63–72.

Gietz RD, Woods RA. Transformation of yeast by lithium acetate/single-stranded carrier DNA/polyethylene glycol method. In: Guthrie C, Fink GR (eds.) *Methods in Enzymology*, vol. 350: Academic Press, 2002,87–96.

Gombert AK, van Maris AJA. Improving conversion yield of fermentable sugars into fuel ethanol in 1st generation yeast-based production processes. *Curr Opin Biotechnol* 2015;**33**:81–86.

Gonçalves DL, Matsushika A, de Sales BB *et al.* Xylose and xylose/glucose co-fermentation by recombinant *Saccharomyces cerevisiae* strains expressing individual hexose transporters. *Enzyme Microb Technol* 2014;**63**:13–20.

Gottardi M, Reifenrath M, Boles E *et al.* Pathway engineering for the production of heterologous aromatic chemicals and their derivatives in *Saccharomyces cerevisiae*: bioconversion from glucose. *FEMS Yeast Res* 2017;**17**: fox035.

Grabowska D, Chelstowska A. The *ALD6* gene product is indispensable for providing NADPH in yeast cells lacking glucose-6-phosphate dehydrogenase activity. *J Biol Chem* 2003;**278**:13984–8.

Haguenauer-Tsapis R, André B. Membrane trafficking of yeast transporters: mechanisms and physiological control of downregulation. In: Boles E, Krämer R (eds). *Molecular Mechanisms Controlling Transmembrane Transport*. Berlin, Heidelberg: Springer, 2004,273–323.

Hamacher T, Becker J, Gárdonyi M *et al.* Characterization of the xylose-transporting properties of yeast hexose transporters and their influence on xylose utilization. *Microbiology* 2002;**148**:2783–8.

Heux S, Cadiere A, Dequin S. Glucose utilization glucose utilization of strains lacking *PGI1* and expressing a transhydrogenase suggests differences in the pentose phosphate capacity among *Saccharomyces cerevisiae* strains. *FEMS Yeast Res* 2008;**8**:217–24.

Hucka M, Finney A, Sauro HM *et al.* The systems biology markup language (SBML): a medium for representation and exchange of biochemical network models. *Bioinformatics* 2003;**19**:524–31.

Huibregtse JM, Yang JC, Beaudenon SL. The large subunit of RNA polymerase II is a substrate of the Rsp5 ubiquitin-protein ligase. *Proc Natl Acad Sci USA* 1997;**94**:3656–61.

Jansen MLA, Bracher JM, Papapetridis I *et al.* *Saccharomyces cerevisiae* strains for second-generation ethanol production: from academic exploration to industrial implementation. *FEMS Yeast Res* 2017;**17**: fox044.

Johansson B, Hahn-Hägerdal B. The non-oxidative pentose phosphate pathway controls the fermentation rate of xylulose but not of xylose in *Saccharomyces cerevisiae* TMB3001. *FEMS Yeast Res* 2002;**2**:277–82.

Kaliszewski P, Zoładek T. The role of Rsp5 ubiquitin ligase in regulation of diverse processes in yeast cells. *Acta Biochim Pol* 2008;**55**:649–62.

Katahira S, Ito M, Takema H *et al.* Improvement of ethanol productivity during xylose and glucose co-fermentation by xylose-assimilating *S. cerevisiae* via expression of glucose transporter Sut1. *Enzyme Microb Technol* 2008;**43**:115–9.

Kim SR, Ha S-J, Wei N *et al.* Simultaneous co-fermentation of mixed sugars: a promising strategy for producing cellulosic ethanol. *Trends Biotechnol* 2012;**30**:274–82.

Klinke HB, Ahring BK, Schmidt AS *et al.* Characterization of degradation products from alkaline wet oxidation of wheat straw. *Bioresource Technol* 2002;**82**:15–26.

Klug L, Daum G. Yeast lipid metabolism at a glance. *FEMS Yeast Res* 2014;**14**:369–88.

Krampe S, Stamm O, Hollenberg CP *et al.* Catabolite inactivation of the high-affinity hexose transporters Hxt6 and Hxt7 of *Saccharomyces cerevisiae* occurs in the vacuole after internalization by endocytosis. *FEBS Lett* 1998;**441**:343–7.

Kuijpers NG, Solis-Escalante D, Bosman L *et al.* A versatile, efficient strategy for assembly of multi-fragment expression vectors in *Saccharomyces cerevisiae* using 60 bp synthetic recombination sequences. *Microb Cell Fact* 2013;**12**:47.

Kuyper M, Harhangi HR, Stave AK *et al.* High-level functional expression of a fungal xylose isomerase: the key to efficient

ethanolic fermentation of xylose by *Saccharomyces cerevisiae*? *FEMS Yeast Res* 2003;**4**:69–78.

Kuyper M, Hartog MMP, Toirkens MJ *et al.* Metabolic engineering of a xylose-isomerase-expressing strain for rapid anaerobic xylose fermentation. *FEMS Yeast Res* 2005a;**5**:399–409.

Kuyper M, Toirkens MJ, Diderich JA *et al.* Evolutionary engineering of mixed-sugar utilization by a xylose-fermenting strain. *FEMS Yeast Res* 2005b;**5**:925–34.

Lee W-J, Kim M-D, Ryu Y-W *et al.* Kinetic studies on glucose and xylose transport in *Saccharomyces cerevisiae*. *Appl Microbiol Biot* 2002;**60**:186–91.

Lopes ML, Paulillo SCdL, Godoy A *et al.* Ethanol production in Brazil: a bridge between science and industry. *Braz J Microbiol* 2016;**47**:64–76.

Lynd LR, Liang X, Biddy MJ *et al.* Cellulosic ethanol: status and innovation. *Curr Opin Biotechnol* 2017;**45**:202–11.

Mangat S, Chandrashekarappa D, McCartney RR *et al.* Differential roles of the glycogen-binding domains of beta subunits in regulation of the Snf1 kinase complex. *Eukaryot Cell* 2010;**9**:173–83.

Mans R, van Rossum HM, Wijsman M *et al.* CRISPR/Cas9: a molecular Swiss army knife for simultaneous introduction of multiple genetic modifications in *Saccharomyces cerevisiae*. *FEMS Yeast Res* 2015;**15**:fov004.

Matsumoto K, Toh-e A, Oshima Y. Isolation and characterization of dominant mutations resistant to carbon catabolite repression of galactokinase synthesis in *Saccharomyces cerevisiae*. *Mol Cell Biol* 1981;**1**:83–93.

Miskovic L, Alff-Tuomala S, Soh KC *et al.* A design–build–test cycle using modeling and experiments reveals interdependencies between upper glycolysis and xylose uptake in recombinant S. cerevisiae and improves predictive capabilities of large-scale kinetic models. *Biotechnol Biofuels* 2017;**10**:166.

Momcilovic M, Iram SH, Liu Y *et al.* Roles of the glycogen-binding domain and Snf4 in glucose inhibition of *SNF1* protein kinase. *J Biol Chem* 2008;**283**:19521–9.

Moysés D, Reis V, Almeida J *et al.* Xylose fermentation by *Saccharomyces cerevisiae*: challenges and prospects. *Int J Mol Sci* 2016;**17**:207.

Nijkamp JF, van den Broek M, Datema E *et al.* De novo sequencing, assembly and analysis of the genome of the laboratory strain *Saccharomyces cerevisiae* CEN.PK113-7D, a model for modern industrial biotechnology. *Microb Cell Fact* 2012;**11**:36.

Nijland JG, Shin HY, Boender LGM *et al.* Improved xylose metabolism by a *CYC8* mutant of *Saccharomyces cerevisiae*. *Appl Environ Microb* 2017;**83**:95–117.

Nijland JG, Shin HY, de Jong RM *et al.* Engineering of an endogenous hexose transporter into a specific D-xylose transporter facilitates glucose-xylose co-consumption in *Saccharomyces cerevisiae*. *Biotechnol Biofuels* 2014;**7**:168.

Nijland JG, Vos E, Shin HY *et al.* Improving pentose fermentation by preventing ubiquitination of hexose transporters in *Saccharomyces cerevisiae*. *Biotechnol Biofuels* 2016;**9**:158.

Özcan S, Johnston M. Function and regulation of yeast hexose transporters. *Microbiol Mol Biol R* 1999;**63**:554–69.

Palmqvist E, Hahn-Hägerdal B. Fermentation of lignocellulosic hydrolysates. II: inhibitors and mechanisms of inhibition. *Bioresource Technol* 2000;**74**:25–33.

Papapetridis I, Goudriaan M, Vázquez Vitali M *et al.* Optimizing anaerobic growth rate and fermentation kinetics in *Saccharomyces cerevisiae* strains expressing Calvin-cycle enzymes for improved ethanol yield. *Biotechnol Biofuels* 2018;**11**:17.

Papapetridis I, van Dijk M, Dobbe APA *et al.* Improving ethanol yield in acetate-reducing *Saccharomyces cerevisiae* by cofactor engineering of 6-phosphogluconate dehydrogenase and deletion of *ALD6*. *Microb Cell Fact* 2016;**15**:67.

Peláez R, Herrero P, Moreno F. Functional domains of yeast hexokinase 2. *Biochem J* 2010;**432**:181–90.

Petit T, Diderich JA, Kruckeberg AL *et al.* Hexokinase regulates kinetics of glucose transport and expression of genes encoding hexose transporters in *Saccharomyces cerevisiae*. *J Bacteriol* 2000;**182**:6815–8.

Raamsdonk LM, Diderich JA, Kuiper A *et al.* Co-consumption of sugars or ethanol and glucose in a *Saccharomyces cerevisiae* strain deleted in theHXK2 gene. *Yeast* 2001;**18**:1023–33.

Rahner A, Schöler A, Martens E *et al.* Dual influence of the yeast Catlp (Snflp) protein kinase on carbon source-dependent transcriptional activation of gluconeogenic genes by the regulatory gene CAT8. *Nucleic Acids Res* 1996;**24**:2331–7.

Reifenberger E, Boles E, Ciriacy M. Kinetic characterization of individual hexose transporters of *Saccharomyces cerevisiae* and their relation to the triggering mechanisms of glucose repression. *Eur J Biochem* 1997;**245**:324–33.

Reznicek O, Facey SJ, de Waal PP *et al.* Improved xylose uptake in *Saccharomyces cerevisiae* due to directed evolution of galactose permease Gal2 for sugar co-consumption. *J Appl Microbiol* 2015;**119**:99–111.

Schmidt MC, McCartney RR. beta-subunits of Snf1 kinase are required for kinase function and substrate definition. *EMBO J* 2000;**19**:4936–43.

Schüller H-J. Transcriptional control of nonfermentative metabolism in the yeast *Saccharomyces cerevisiae*. *Curr Genet* 2003;**43**:139–60.

Shcherbik N, Pestov DG. The ubiquitin ligase Rsp5 is required for ribosome stability in *Saccharomyces cerevisiae*. *RNA* 2011;**17**:1422–8.

Shen M-H, Song H, Li B-Z *et al.* Deletion of D-ribulose-5-phosphate 3-epimerase (*RPE1*) induces simultaneous utilization of xylose and glucose in xylose-utilizing *Saccharomyces cerevisiae*. *Biotechnol Lett* 2015;**37**:1031–6.

Shen Y, Chen X, Peng B *et al.* An efficient xylose-fermenting recombinant *Saccharomyces cerevisiae* strain obtained through adaptive evolution and its global transcription profile. *Appl Microbiol Biot* 2012;**96**:1079–91.

Shin HY, Nijland JG, de Waal PP *et al.* An engineered cryptic Hxt11 sugar transporter facilitates glucose–xylose co-consumption in *Saccharomyces cerevisiae*. *Biotechnol Biofuels* 2015;**8**:176.

Solis-Escalante D, Kuijpers NGA, Bongaerts N *et al. amdSYM*, a new dominant recyclable marker cassette for *Saccharomyces cerevisiae*. *FEMS Yeast Res* 2013;**13**:126–39.

Subtil T, Boles E. Competition between pentoses and glucose during uptake and catabolism in recombinant *Saccharomyces cerevisiae*. *Biotechnol Biofuels* 2012;**5**:14.

Tehlivets O, Scheuringer K, Kohlwein SD. Fatty acid synthesis and elongation in yeast. *BBA-Mol Cell Biol L* 2007;**1771**:255–70.

van den Brink J, Akeroyd M, van der Hoeven R *et al.* Energetic limits to metabolic flexibility: responses of *Saccharomyces cerevisiae* to glucose-galactose transitions. *Microbiology* 2009;**155**:1340–50.

van Maris AJA, Abbott DA, Bellissimi E *et al.* Alcoholic fermentation of carbon sources in biomass hydrolysates by *Saccharomyces cerevisiae*: current status. *Anton Leeuw* 2006;**90**:391–418.

Verduyn C, Postma E, Scheffers WA *et al.* Physiology of *Saccharomyces cerevisiae* in anaerobic glucose-limited chemostat cultures. *Microbiology* 1990;**136**:395–403.

Verduyn C, Postma E, Scheffers WA *et al*. Effect of benzoic acid on metabolic fluxes in yeasts: a continuous-culture study on the regulation of respiration and alcoholic fermentation. *Yeast* 1992;**8**:501–17.

Verhoeven MD, Lee M, Kamoen L *et al*. Mutations in *PMR1* stimulate xylose isomerase activity and anaerobic growth on xylose of engineered *Saccharomyces cerevisiae* by influencing manganese homeostasis. *Sci Rep* 2017;**7**:46155.

Vincent O, Carlson M. Sip4, a Snf1 kinase-dependent transcriptional activator, binds to the carbon source-responsive element of gluconeogenic genes. *EMBO J* 1998;**17**:7002–8.

Vincent O, Carlson M. Gal83 mediates the interaction of the Snf1 kinase complex with the transcription activator Sip4. *EMBO J* 1999;**18**:6672–81.

Vincent O, Townley R, Kuchin S *et al*. Subcellular localization of the Snf1 kinase is regulated by specific beta subunits and a novel glucose signaling mechanism. *Gene Dev* 2001;**15**:1104–14.

Wei N, Oh EJ, Million G *et al*. Simultaneous utilization of cellobiose, xylose, and acetic acid from lignocellulosic biomass for biofuel production by an engineered yeast platform. *ACS Synth Biol* 2015;**4**:707–13.

Westman JO, Bonander N, Taherzadeh MJ *et al*. Improved sugar co-utilisation by encapsulation of a recombinant *Saccharomyces cerevisiae* strain in alginate-chitosan capsules. *Biotechnol Biofuels* 2014;**7**:102.

Wiatrowski HA, van Denderen BJW, Berkey CD *et al*. Mutations in the Gal83 glycogen-binding domain activate the Snf1/Gal83 kinase pathway by a glycogen-independent mechanism. *Mol Cell Biol* 2004;**24**:352–61.

Wisselink HW, Toirkens MJ, del Rosario Franco Berriel M *et al*. Engineering of *Saccharomyces cerevisiae* for efficient anaerobic alcoholic fermentation of l-arabinose. *Appl Environ Microb* 2007;**73**:4881–91.

Wisselink HW, Toirkens MJ, Wu Q *et al*. Novel evolutionary engineering approach for accelerated utilization of glucose, xylose, and arabinose mixtures by engineered *Saccharomyces cerevisiae* strains. *Appl Environ Microb* 2009;**75**:907–14.

Wisselink HW, van Maris AJA, Pronk JT. WO/2014/195522.Polypeptides with permease activity. 2015.

Zhou H, Cheng J-s, Wang BL *et al*. Xylose isomerase overexpression along with engineering of the pentose phosphate pathway and evolutionary engineering enable rapid xylose utilization and ethanol production by *Saccharomyces cerevisiae*. *Metab Eng* 2012;**14**:611–22.